

**UNCLASSIFIED**

---

**AD 268 948**

*Reproduced  
by the*

**ARMED SERVICES TECHNICAL INFORMATION AGENCY  
ARLINGTON HALL STATION  
ARLINGTON 12, VIRGINIA**



---

**UNCLASSIFIED**

NOTICE: When government or other drawings, specifications or other data are used for any purpose other than in connection with a definitely related government procurement operation, the U. S. Government thereby incurs no responsibility, nor any obligation whatsoever; and the fact that the Government may have formulated, furnished, or in any way supplied the said drawings, specifications, or other data is not to be regarded by implication or otherwise as in any manner licensing the holder or any other person or corporation, or conveying any rights or permission to manufacture, use or sell any patented invention that may in any way be related thereto.

CATALOGED BY ASTIA

AS AD NO. \_\_\_\_\_

268948

62-155  
NOX

# MEASUREMENT OF WIND SHEAR

## FINAL REPORT

Covering period 1 December 1959 to 30 June 1961

Signal Corps Contract No. DA 36-039 SC-84950  
File No. 40118-PM-60-91-91 (1526M)  
PR and C No. 61-ELS/R-1714

U. S. Army Signal Engineering Laboratories  
Fort Monmouth, N. J.

Submitted by: UNITED RESEARCH INCORPORATED  
Physical Sciences Division  
138 Alewife Brook Parkway  
Cambridge 40, Massachusetts

RECEIVED

<p>AD _____ Accession No. _____</p> <p>United Research Incorporated, Cambridge, Massachusetts MEASUREMENT OF WIND SHEAR</p> <p>Final Report, 1 December 1959 - 30 June 1961, 40 pp-Illustrations (Contract No. DA 36-039 SC-84950) PR and C No. 61-ELS/R-1714</p> <p>Description of wind shear measurement system. Final configuration of probe. Telemetry system description. Computer logic and programming for data reduction. Field testing. Recommendations for future testing and developments.</p>	<p>UNCLASSIFIED</p> <ol style="list-style-type: none"> <li>1. Wind velocity</li> <li>2. Wind shear</li> <li>3. Aerodynamic tuning theory</li> <li>4. Telemetering techniques</li> </ol>	<p>AD _____ Accession No. _____</p> <p>United Research Incorporated, Cambridge, Massachusetts MEASUREMENT OF WIND SHEAR</p> <p>Final Report, 1 December 1959 - 30 June 1961, 40 pp-Illustrations (Contract No. DA 36-039 SC-84950) PR and C No. 61-ELS/R-1714</p> <p>Description of wind shear measurement system. Final configuration of probe. Telemetry system description. Computer logic and programming for data reduction. Field testing. Recommendations for future testing and developments.</p>	<p>UNCLASSIFIED</p> <ol style="list-style-type: none"> <li>1. Wind velocity</li> <li>2. Wind shear</li> <li>3. Aerodynamic tuning theory</li> <li>4. Telemetering techniques</li> </ol>
<p>AD _____ Accession No. _____</p> <p>United Research Incorporated, Cambridge, Massachusetts MEASUREMENT OF WIND SHEAR</p> <p>Final Report, 1 December 1959 - 30 June 1961, 40 pp-Illustrations (Contract No. DA 36-039 SC-84950) PR and C No. 61-ELS/R-1714</p> <p>Description of wind shear measurement system. Final configuration of probe. Telemetry system description. Computer logic and programming for data reduction. Field testing. Recommendations for future testing and developments.</p>	<p>UNCLASSIFIED</p> <ol style="list-style-type: none"> <li>1. Wind velocity</li> <li>2. Wind shear</li> <li>3. Aerodynamic tuning theory</li> <li>4. Telemetering techniques</li> </ol>	<p>AD _____ Accession No. _____</p> <p>United Research Incorporated, Cambridge, Massachusetts MEASUREMENT OF WIND SHEAR</p> <p>Final Report, 1 December 1959 - 30 June 1961, 40 pp-Illustrations (Contract No. DA 36-039 SC-84950) PR and C No. 61-ELS/R-1714</p> <p>Description of wind shear measurement system. Final configuration of probe. Telemetry system description. Computer logic and programming for data reduction. Field testing. Recommendations for future testing and developments.</p>	<p>UNCLASSIFIED</p> <ol style="list-style-type: none"> <li>1. Wind velocity</li> <li>2. Wind shear</li> <li>3. Aerodynamic tuning theory</li> <li>4. Telemetering techniques</li> </ol>

<p>AD _____ Accession No. _____</p> <p>United Research Incorporated, Cambridge, Massachusetts MEASUREMENT OF WIND SHEAR</p> <p>Final Report, 1 December 1959 - 30 June 1961, 40 pp-illustrations (Contract No. DA 36-039 SC-84950) PR and C No. 61-ELS/R-1714</p> <p>Description of wind shear measurement system. Final configuration of probe. Telemetry system description. Computer logic and programming for data reduction. Field testing. Recommendations for future testing and developments.</p>	<p>UNCLASSIFIED</p> <ol style="list-style-type: none"> <li>1. Wind velocity</li> <li>2. Wind shear</li> <li>3. Aerodynamic tuning theory</li> <li>4. Telemetering techniques</li> </ol>
<p>AD _____ Accession No. _____</p> <p>United Research Incorporated, Cambridge, Massachusetts MEASUREMENT OF WIND SHEAR</p> <p>Final Report, 1 December 1959 - 30 June 1961, 40 pp-illustrations (Contract No. DA 36-039 SC-84950) PR and C No. 61-ELS/R-1714</p> <p>Description of wind shear measurement system. Final configuration of probe. Telemetry system description. Computer logic and programming for data reduction. Field testing. Recommendations for future testing and developments.</p>	<p>UNCLASSIFIED</p> <ol style="list-style-type: none"> <li>1. Wind velocity</li> <li>2. Wind shear</li> <li>3. Aerodynamic tuning theory</li> <li>4. Telemetering techniques</li> </ol>
<p>AD _____ Accession No. _____</p> <p>United Research Incorporated, Cambridge, Massachusetts MEASUREMENT OF WIND SHEAR</p> <p>Final Report, 1 December 1959 - 30 June 1961, 40 pp-illustrations (Contract No. DA 36-039 SC-84950) PR and C No. 61-ELS/R-1714</p> <p>Description of wind shear measurement system. Final configuration of probe. Telemetry system description. Computer logic and programming for data reduction. Field testing. Recommendations for future testing and developments.</p>	<p>UNCLASSIFIED</p> <ol style="list-style-type: none"> <li>1. Wind velocity</li> <li>2. Wind shear</li> <li>3. Aerodynamic tuning theory</li> <li>4. Telemetering techniques</li> </ol>
<p>AD _____ Accession No. _____</p> <p>United Research Incorporated, Cambridge, Massachusetts MEASUREMENT OF WIND SHEAR</p> <p>Final Report, 1 December 1959 - 30 June 1961, 40 pp-illustrations (Contract No. DA 36-039 SC-84950) PR and C No. 61-ELS/R-1714</p> <p>Description of wind shear measurement system. Final configuration of probe. Telemetry system description. Computer logic and programming for data reduction. Field testing. Recommendations for future testing and developments.</p>	<p>UNCLASSIFIED</p> <ol style="list-style-type: none"> <li>1. Wind velocity</li> <li>2. Wind shear</li> <li>3. Aerodynamic tuning theory</li> <li>4. Telemetering techniques</li> </ol>

MEASUREMENT OF WIND SHEAR

FINAL REPORT

Covering period 1 December 1959 to 30 June 1961

COMPONENT CONSTRUCTION AND TESTING

Signal Corps Technical Requirements No. SCL-5334A  
dated March 4, 1958

Signal Corps Contract No. DA-36-039 SC-84950  
File No. 40118-PM-60-91-91 (1526M)  
PR and C No. 61-ELS/R-1714

Prepared by:

*Thomas E. Beling*  
Thomas E. Beling

*Donald R. Benders*  
Donald R. Benders

*Roland L. Plante*  
Roland L. Plante

## TABLE OF CONTENTS

	<u>Page</u>
Purpose . . . . .	1
Abstract . . . . .	ii
Publications, Lectures, Reports and Conferences. . . . .	iii
<u>Chapter</u>	
1      Introduction . . . . .	1
2      Probe Description . . . . .	2
3      Ground Support Equipment . . . . .	20
4      Testing . . . . .	39
5      Conclusions . . . . .	40

## PURPOSE

This contract was for the field testing of the wind shear probe developed under Signal Corps Contract DA-36-039 SC-75064.

This report describes the efforts to calibrate and test all components in the system with a brief description of field testing conducted at White Sands Missile Range, New Mexico.



## ABSTRACT

Chapter 1 describes the background of the wind shear measuring technique.

Chapter 2 describes the mechanical construction of the wind shear probe and gives some of the design criteria for the various sensors. Also described is the instrumentation package which contains the telemetering link and the electronic circuits necessary to measure the various parameters, i.e., wind acceleration, probe velocity and probe position in space.

Chapter 3 describes the ground support equipment. This includes the AN/GMD-1A receiver, a ground logic and tape recorder. The description of these items is lengthy and includes complete description of signal flow through the various circuits.

Chapter 4 describes the various in-plant tests conducted to prove (1) reliability of the equipment, and (2) accuracy of the equipment. This chapter also describes some of the field tests conducted at White Sands Missile Range.

## PUBLICATIONS, LECTURES, REPORTS, AND CONFERENCES

- (a) Publications: None
- (b) Lectures: None
- (c) Reports:
  - 1) First Quarterly Report, Measurement of Wind Shear covering period 1 May 1958 to 30 September 1958
  - 2) Second Quarterly Report, Measurement of Wind Shear covering period 1 October 1958 to 30 December 1958
  - 3) Third Quarterly Report, Measurement of Wind Shear covering period 1 January 1959 to 31 May 1959
  - 4) Fourth Quarterly Report, Measurement of Wind Shear covering period 1 June 1959 to 31 August 1959
  - 5) Fifth Quarterly Report, Measurement of Wind Shear covering period 1 September 1959 to 30 November 1959
- (d) Conferences: None

## CHAPTER 1

### INTRODUCTION

This report describes a wind shear measuring system developed by United Research Incorporated, under Contract No. DA 36-039 SC-84950.

The wind shear probe - the critical component of the system - consists of an 18 pound, 77 inch long cylinder, 6 inches in diameter, with two concentric cylindrical wing surfaces, 24 inches and 18 inches in diameter, respectively. This probe is aerodynamically tuned to fall vertically regardless of wind forces. This tuning allows the measurement of horizontal wind forces to be reduced to a measurement of horizontal accelerations experienced by the probe during its fall. A knowledge of probe azimuthal orientation and altitude is required in order to determine the direction and magnitude of wind forces as a function of altitude - i.e., wind shear. The probe is instrumented to measure horizontal accelerations in two quadrature axes, azimuthal orientation, and altitude, and to transmit this information continuously during a drop.

Telemetered data in the form of a hybrid PDM/PPM code is received by the ground station. These data are modified by the ground logic system to a form suitable for reduction by an IBM 704 computer.

## CHAPTER 2

### PROBE DESCRIPTION

The three basic requirements of the wind shear probe structure are: (1) low density, (2) sufficient rigidity to withstand imposed wind loads with no effective change in aerodynamic configuration, and (3) dimensional symmetry and reproducibility.

Low structural density is required for the following reasons. First, a high probe drag-to-weight ratio avoids sonic velocities in free fall from high launching altitudes; second, a lightweight probe air frame simplifies the necessary forward center-of-gravity location with minimum nose ballast; third, a low mass results in a shorter wind response distance, thus permitting more accurate wind tracking with correspondingly less stringent demands upon dynamic response expansion operations; and fourth, as discussed in the Second Quarterly Report, the stability margin and aerodynamic tuning tolerance both become greater as probe density is decreased.

#### 2.1 Structure and Aerodynamic Design

To meet the basic requirements already noted, it was found that two techniques were available; aluminum honeycomb sandwich construction, and molded expanded polystyrene foam plastic. The aluminum honeycomb sandwich structures provide greater rigidity than foam plastic construction, and were therefore used for the highly stressed cylindrical forward wing and tail wing, and the body sections. On the other hand, foam plastic is more efficiently formed to complex shapes and was used for the nose section, wing struts, and body section bulkheads. Details concerning the choice of construction techniques may be found in the Second and Third Quarterly Reports.

Although the density of the final field-test version is low enough to permit launching from 50,000 feet, it is essential that the weight be reduced if probes are to be launched from greater altitudes. Such a density reduction would increase the accuracy of the wind shear measuring system as well as increase the altitude range over which the system might be employed. This density reduction may be effected by decreasing the physical dimensions of the probe and substituting expanded polystyrene foam plastic for honeycomb construction in several sections of the probe structure, notably, the body and tail wing.

The aerodynamic considerations underlying the design of the probe are based on the theory of the tuned probe, as set forth by Prof. Larrabee in the

Second Quarterly Report. The cylindrical wings and body dimensions with the estimated mass distribution of the airframe structure, instrument package, and parachute recovery system, would result in a center of gravity about two inches ahead of the center of pressure. Accurate tuning is then achieved with a minimum of ballast. However, the field-test probe was tail heavy and required considerable ballast to properly tune the vehicle. Axial symmetry is necessary in order to compensate for rotation of the probe during descent. Further, the structural strength of the air frame was predicated on the expected aerodynamic loads encountered in flight.

## 2.2 Sensors

Information telemetered to the ground equipment is sensed by two accelerometers, a magnetometer, and a pressure sensitive baroswitch. The orthogonal arrangement of two single-axis accelerometers defines the magnitude and direction of local horizontal wind shear with respect to the probe. The magnetometer provides information of the orientation of the probe with respect to earth-fixed geomagnetic coordinates. These data then define the magnitude and direction of the horizontal wind shear with respect to earth coordinates. The barometric pressure sensor is an AN/AMT-4 standard radiosonde unit used to measure probe altitude. A second unit is used as the release point switch for parachute deployment.

### 2.2.1 Accelerometers

The maximum vertical velocity of the wind shear probe is 750 feet per second at an altitude of approximately 85,000 feet when the probe is launched from 100,000 feet. At this velocity, a wind shear across a zone thickness of ten feet will have a fundamental frequency of 75 cycles per second. To reduce the complexity of the data, the dynamic effects of the accelerometer performance can be made negligible if the undamped natural frequency is at least an order of magnitude greater than the highest frequency to be measured. In this instance it should be at least 750 cycles per second. The displacement of the seismic element with respect to the case for a constant acceleration is given by the expression

$$X_{[ca-m]} = \frac{1}{\omega_n^2} a$$

where

$\omega_n$  = undamped natural frequency of seismic mass spring system  
(in radians per second)

$a$  = input acceleration

$X_{[ca-m]}$  = displacement of mass with respect to case

As outlined in Chapter 6, Third Quarterly Report, the uncertainty in measuring acceleration should be no greater than .001 g. Substituting this acceleration

into the expression for the displacement yields  $X_{[ca-m]} = 1.76 \times 10^{-8}$  inches, a quantity which is extremely difficult to measure reliably.

When the minimum zone thickness is taken as fifteen feet, the fundamental component of wind shear is 50 cycles per second. Using a factor of two, rather than ten, as the ratio of the accelerometer undamped natural frequency and the highest frequency to be measured gives 100 cycles per second. The dynamic limitations of the accelerometer are further minimized by providing a damping ratio of about 0.7. Now an acceleration of .001 g will cause a displacement of the seismic mass of approximately one-millionth of an inch, a quantity which can be measured reliably, though with some difficulty.

Initially, a polar accelerometer design was investigated which would respond to an acceleration vector lying in the plane of the sensing element. A design was completed but was not produced since a convenient method for reading out the vector orientation with respect to the probe was not available. This approach was subsequently abandoned.

The accelerometer design used in the wind shear probe is a single axis, variable reluctance type device. It consists of a U-shaped high permeability (5000 gauss/oersted) ferrite core around which is wound a coil. The seismic element is a ferrite bar supported on a cantilever plate spring. The approximate volume is 1 in<sup>3</sup>. Figures 2.1 and 2.2 show the accelerometer and the arrangement in assembly, respectively. Only a single accelerometer is shown for clarity.

When an acceleration is applied, the seismic element undergoes a displacement and varies the gap between the stationary U-core and the bar. The resultant change in reluctance is a measure of the acceleration applied. In the wind shear probe, the accelerometer forms the inductive portion of an LC tank circuit. This circuit is pulsed by a signal initiated by the azimuth indicator. The resulting damped electrical transient response or ringing of the LC network is used as a measure of acceleration as follows. The time for the first zero crossing, or the first half cycle, of the transient is a measure of the tank circuit inductance which is related in turn to the existing gap, and, hence to the applied acceleration. Suitable circuitry is included in the readout which suppresses all but the first half cycle to facilitate measurement of the first half cycle time. Figure 2.3 is a graphic representation of the read out for two values of applied acceleration.

The magnitude of  $T_1$  and  $T_2$  are measured and, by calibration, indicate the magnitude of the applied acceleration.

The resolution capability of this accelerometer system is dependent on the time resolution capability of the associated readout circuitry. A resolution of 1 microsecond with the unit used in the wind shear probe provides a

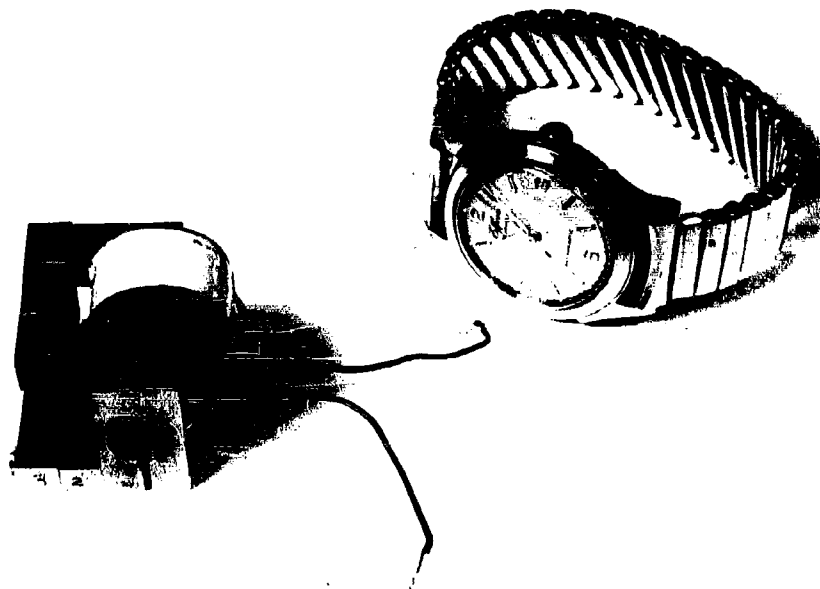


Figure 2.1 Photograph of Accelerometer

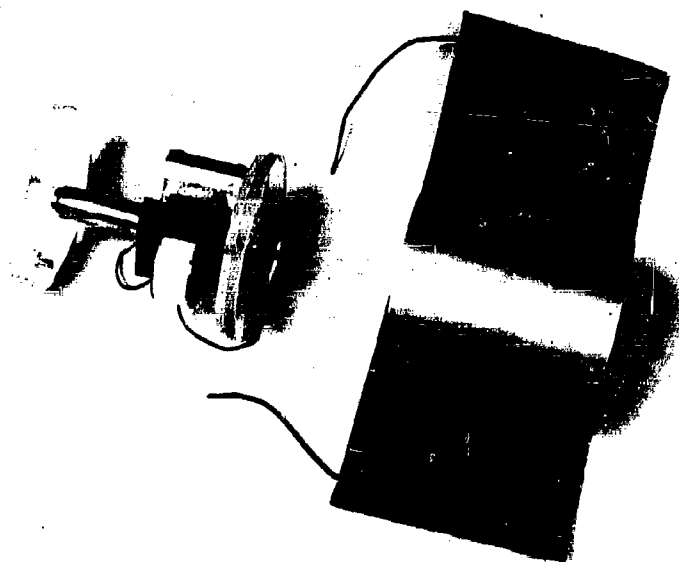


Figure 2.2 Photograph of Accelerometer in Assembly

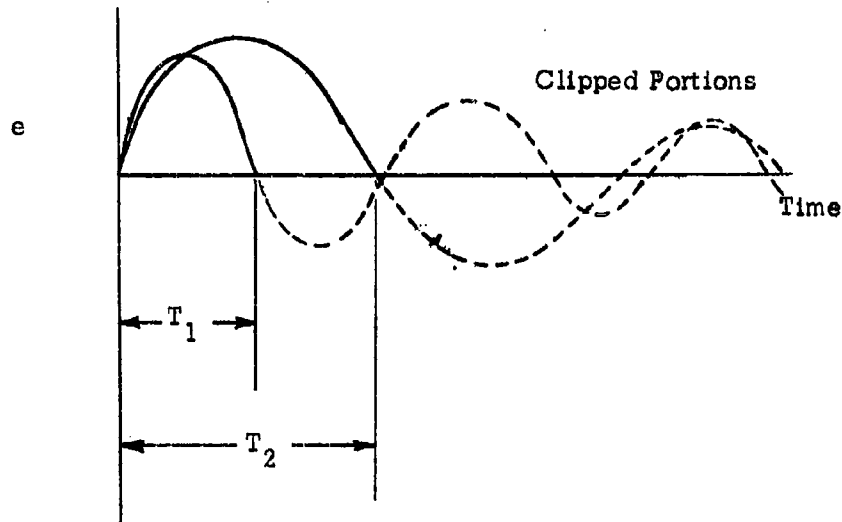


Figure 2.3 Accelerometer Output Waveforms

measure of .003 g of acceleration. Damping is provided by immersing the array, including capacitors, in a fluid whose viscosity is 6.00 centistokes at 0° F. At operating temperature, a damping ratio of about 0.7 is achieved.

Preliminary circuit checkout disclosed that the capacitors which are part of the accelerometer tank circuit were temperature sensitive. Stable operation could be maintained only through environmental temperature control. Consequently, a 12-volt heating unit, or blanket, was wrapped around the array container, which house the capacitors, and is connected to a switching thermostat to control the temperature at  $92^{\circ} \pm 1.5^{\circ} \text{ F}$ .

The accelerometer array was installed in the probe instrument package and the probe mounted on a tilt table vertically to simulate in-flight attitude. The probe was rotated until the axis of the accelerometer was orthogonal to the pivot axis of the table. The angle of tilt is a measure of the local gravitational acceleration, i.e.,  $a = g \sin \theta$  where  $a$  = acceleration applied to seismic mass,  $g$  = local gravitational acceleration, and  $\theta$  = angle of tilt from the vertical. The corresponding time in microseconds was recorded for different tilt angles up to 30° or 0.5 g. Figures 2.4 and 2.5 show the resultant calibration curves for a single, two accelerometer array.

#### 2.2.2 Magnetometer

Two of the quantities which must be measured during a descent of the wind shear probe are the vertical air speed and the azimuth orientation of the



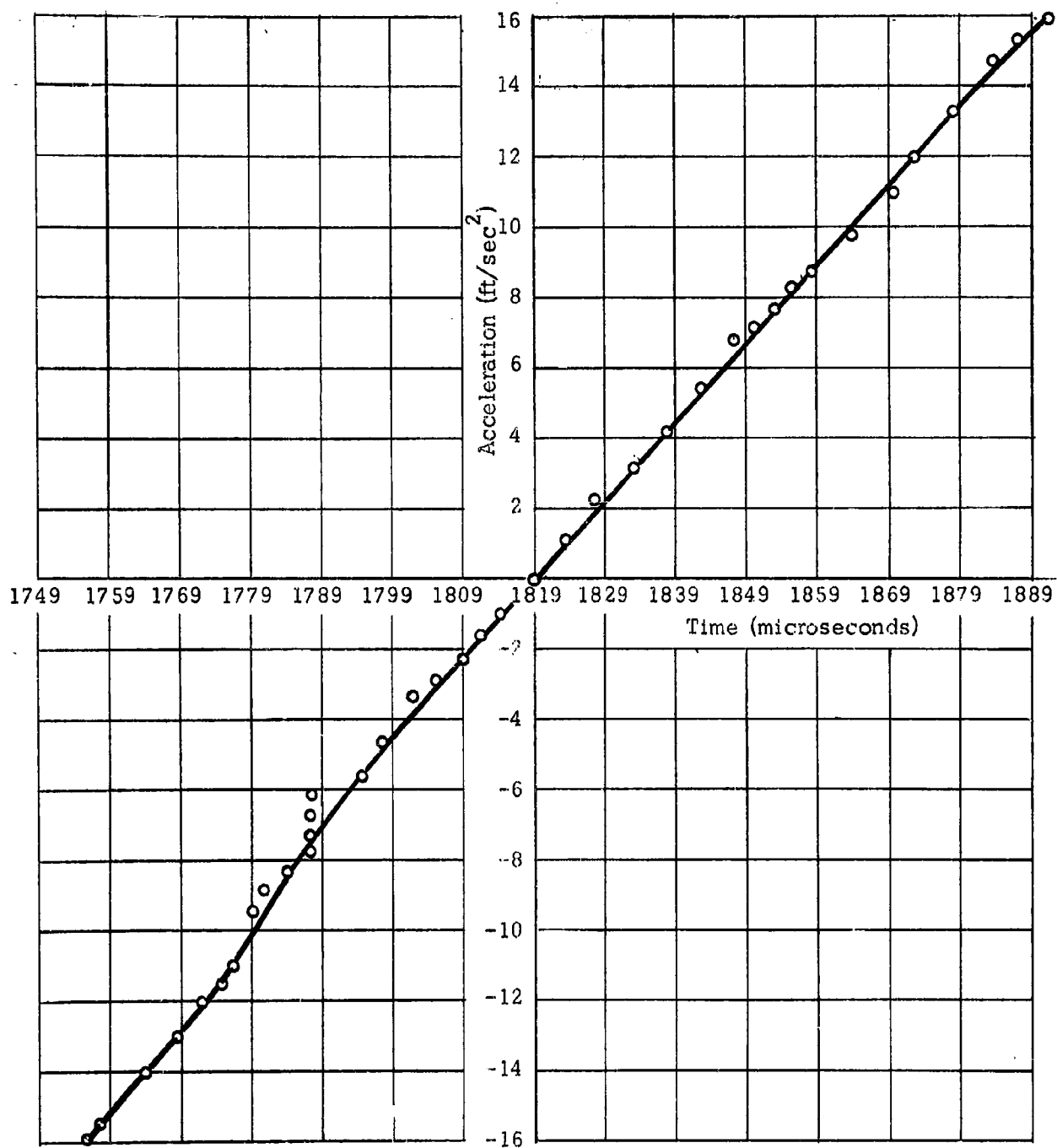


Figure 2.4 Graph of Acceleration of Probe No. 1

X-Axis vs. Time

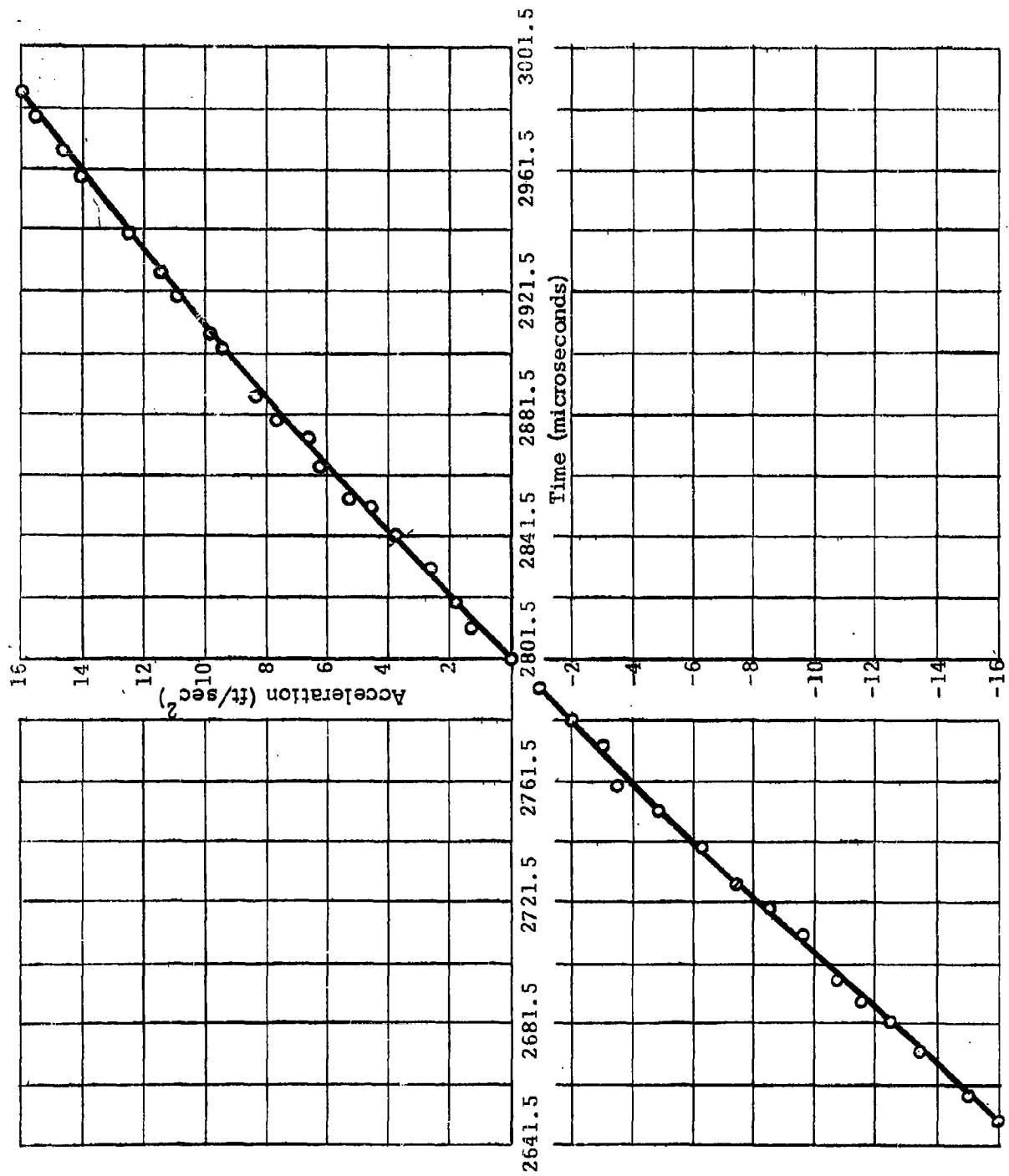


Figure 2.5 Graph of Acceleration of Probe No. 1

Y-Axis vs. Time

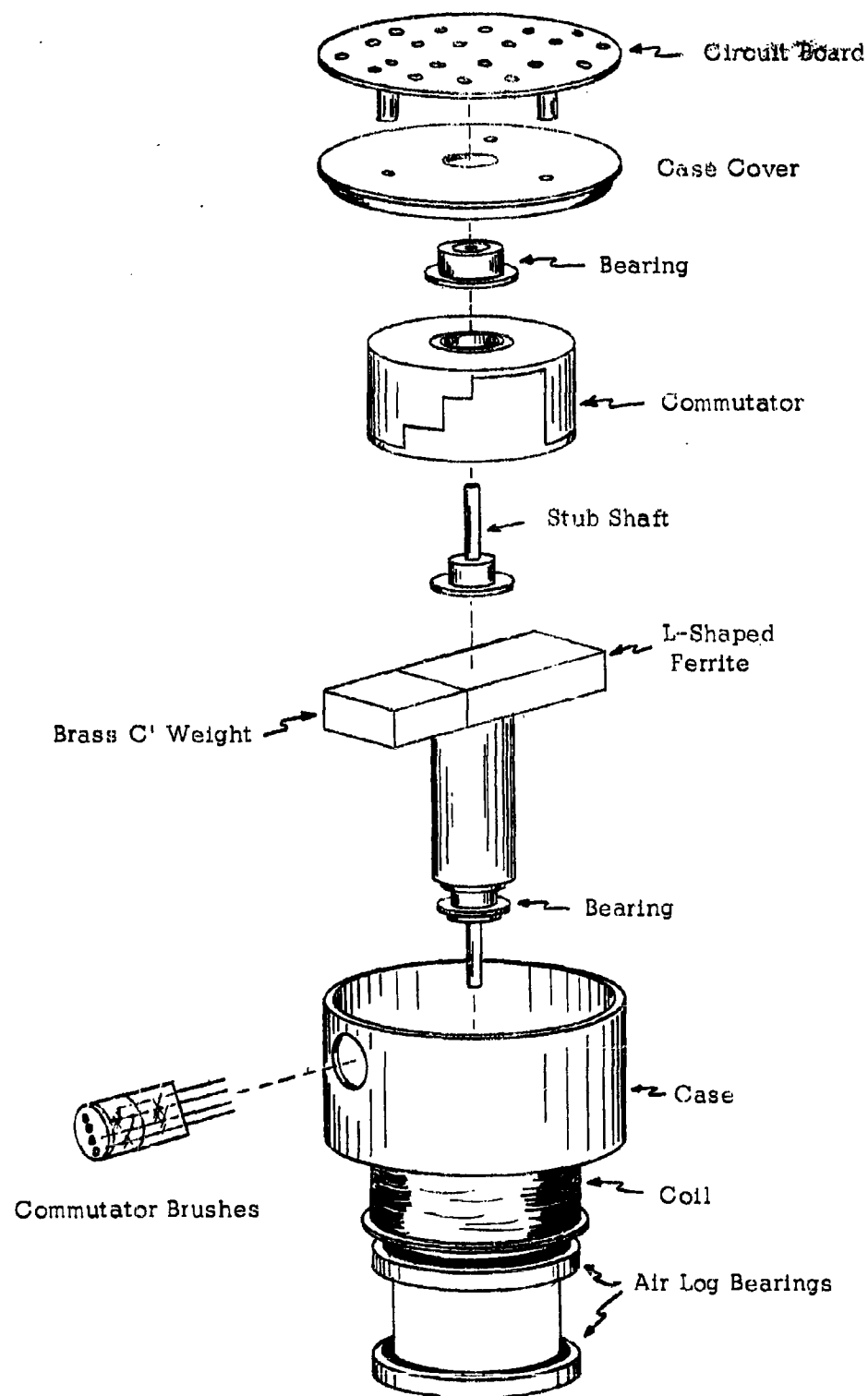


Figure 2.6 Exploded View of Azimuth Indicator

vehicle with respect to the earth. The vertical air speed of the probe is one of the quantities which directly determines the wind shear and so must be measured with precision. Azimuth orientation of the probe with respect to the earth is the only manner in which the direction of wind shear may be determined. Since the probe rotates during descent it becomes necessary to generate azimuth information to relate the accelerometer output to the wind shear direction.

The azimuth indicator generates a single electrical signal which simultaneously indicates the vertical air speed of the wind shear probe, its azimuth orientation with respect to the earth's magnetic field.

The device as shown in Figure 2.6 consists of a high permeability L-shaped core which is rotated about a vertical axis within a coil by an air screw mounted on the nose of the wind shear probe. By virtue of its L-shape, horizontal lines of force of the earth's magnetic field are caused to bend vertically through the coil. As the core rotates the magnetic flux passes through the coil first in one direction and then in the other. The reversing flux induces a sinusoidally varying voltage in the coil as shown in Figure 2.7.

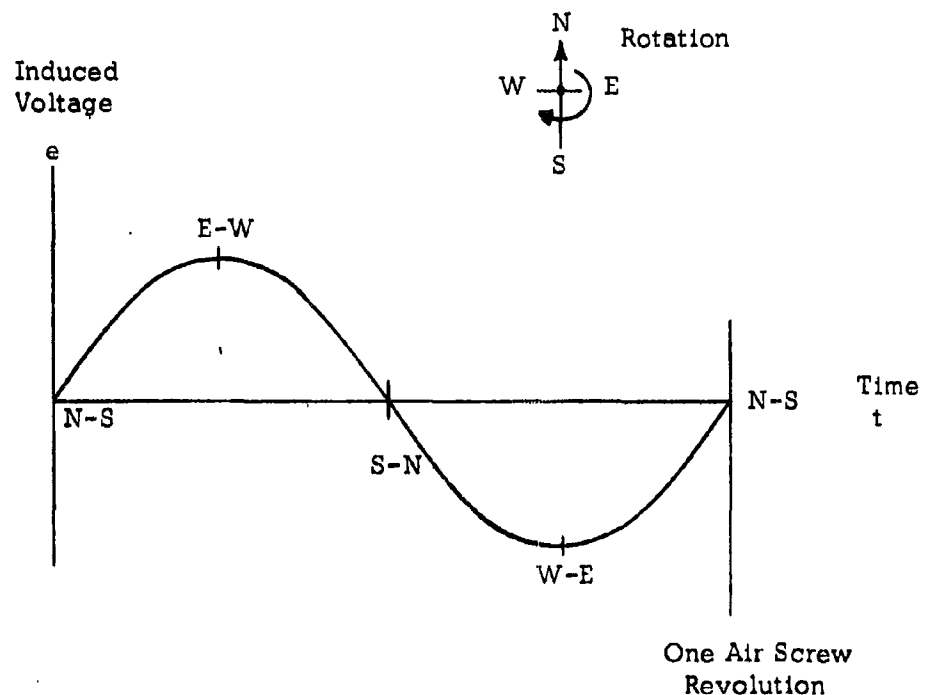


Figure 2.7 Magnetometer Induced Voltage Waveform

The induced voltage in the coil is independent of the wind shear probe orientation since any rotation of the coil, which is fixed to the vehicle, around the core results in no voltage change.

Originally, it was intended to determine probe orientation by shorting out the coil with a rotating shunt fixed to the core so that each time the core makes one complete revolution with respect to the probe, the azimuth indicator voltage is momentarily reduced to zero. Figure 2.8 shows the form of the indicator voltage and the manner in which angular velocity of the air log and orientation of the wind shear probe may be determined from it.

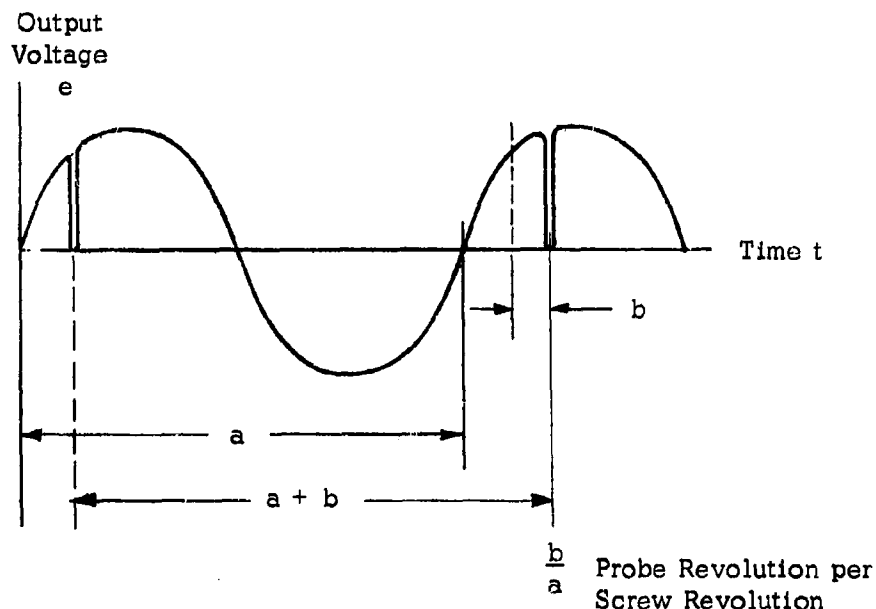


Figure 2.8 Velocity Determination of Wind Shear Probe

Knowing the effective pitch of the air screw and its angular velocity, the axial velocity of the probe is found from the expression

$$V_{\text{axial}} = p_e \times f$$

where

$p_e$  = effective pitch (in feet/revolution)

$f$  = azimuth indicator signal frequency (in rev/sec)

In the final design the coil output is fed to a two-stage squaring amplifier, then inverted and used to trigger a north-south pulse forming circuit. These pulses determine precisely the north-south crossing of the azimuth indicator core. A reference, or case, pulse initiated by a core mounted commutator and a case mounted brush arrangement provides the switching action which enables the probe orientation and the air log angular velocity to be determined. In the telemetering cycle, additional pulses occur which are identified and recorded by suitable ground logic and recording equipment. This additional information is not shown. The commutator performs additional functions. It became apparent that considerable simplification could be effected in the various delay circuits required for telemetering if the commutator were made to produce pulses through brush contact which would initiate the beginning as well as several parts of each data transmission cycle. This was a modification of the original interrupter mechanism whose sole function was to momentarily short the azimuth indicator signal.

### 2.2.3 Barometric pressure

Altitude of the probe above mean sea level is sensed by an AN/AMT-4A barometric pressure sensor used in standard radiosonde systems.

## 2.3 Data Encoding

The data from the wind shear probe are encoded into the form of both pulse duration modulation (PDM) and pulse position modulation (PPM). The basic timing for the data encoder is the rotation of the air log spinner, which is mechanically coupled to the magnetometer and the timing commutator. Therefore, the length of a data frame depends upon the spinner rotation rate. The data transmitted are:

- 1) Barometric altitude
- 2) Azimuthal orientation
- 3) X acceleration
- 4) Y acceleration

### 2.3.1 Timing

A timing diagram of a data frame as transmitted by the wind shear probe is shown below:

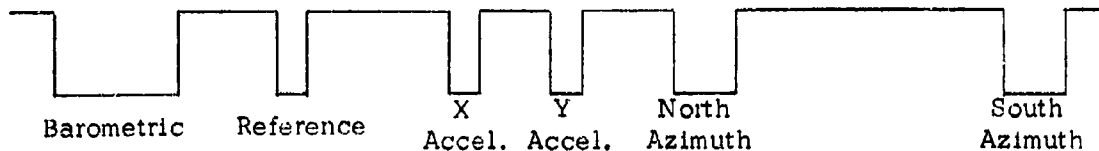
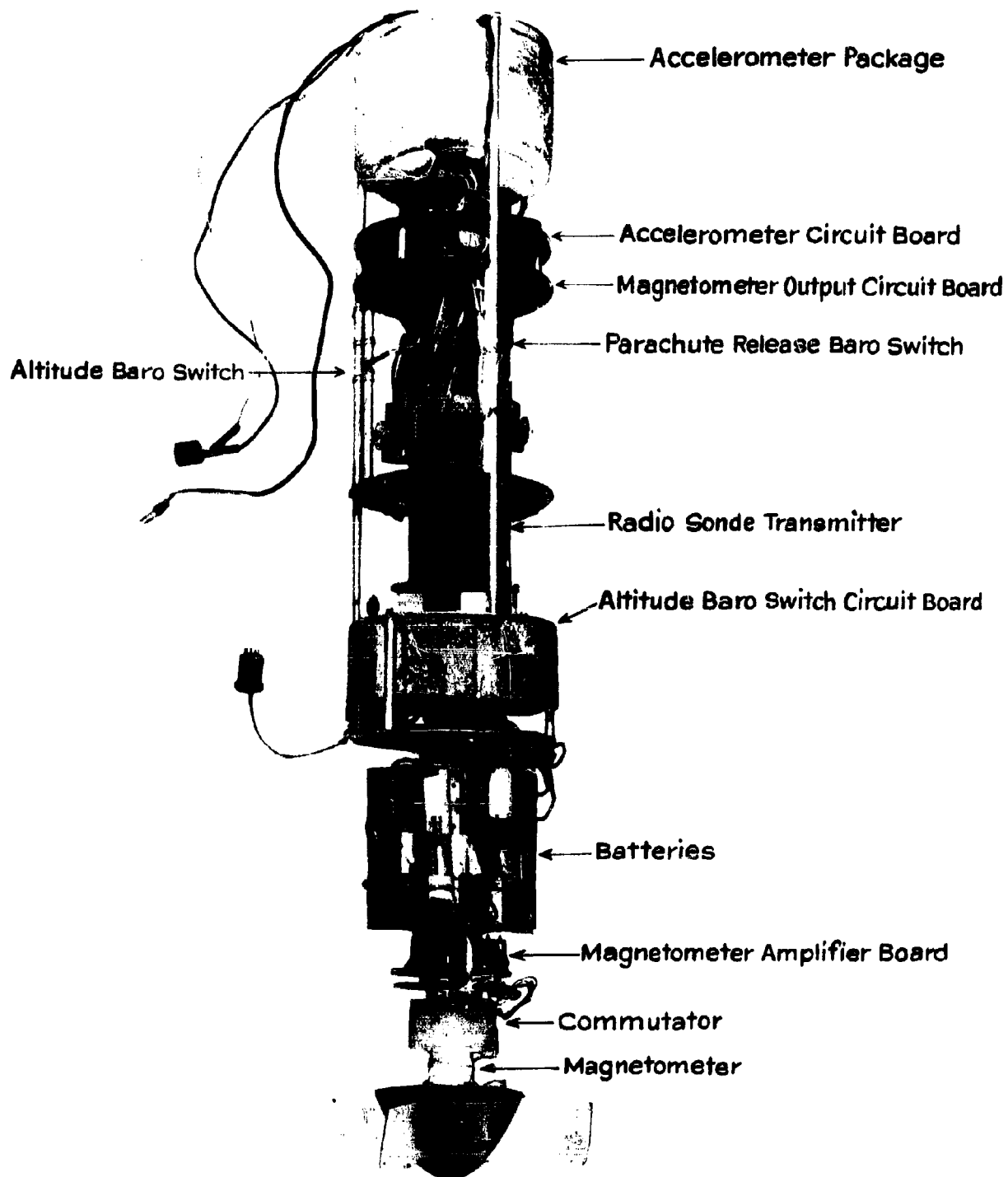


Figure 2.9 Wind Shear Probe Pulse Train



Wind Shear Probe Instrument Package

The total frame time is approximately 14 to 70 milliseconds, depending upon the speed of rotation of the air log.

Successive steps on the commutator blank the azimuth channel, trigger the baro pulse, and trigger the reference pulse and accelerometer read out.

### 2.3.2 Baro pulse channel

The baro pulse multivibrator is triggered by the commutator and generates a pulse with four possible widths - 175, 225, 275, or 325 microseconds. The pulse width is determined by precision capacitors switched into the baro multivibrator by the baro switch. (See Figure 2.10.) The negative going pulse output of the baro multivibrator is connected through a diode Or gate to the base of transistor Q24. During the baro pulse time, Q24 is saturated and delivers a positive pulse to the base of Q23, the modulator.

### 2.3.3 Accelerometer channel

As described in Section 2.2.1, horizontal acceleration of the wind shear probe is sensed as a change in the inductance of the accelerometer coils. The accelerometer readout circuitry translates this change in inductance to a position modulation of the accelerometer pulses with respect to a reference pulse.

When the commutator rotates to step 3, accelerometer readout, capacitors C1 and C2, which have been charged to -12 volts through R1, have one terminal connected to ground. This places a voltage across the accelerometers in a direction to cause conduction of CR1 and CR2. The resulting RLC circuit is underdamped and tends to oscillate sinusoidally. After the first half cycle of oscillation, CR1 and CR2 are cut off, and the energy remaining in the circuits is dissipated in R4 and R5. Thus, the voltages appearing across the output terminals of the accelerometer package consists of a half cycle of a sine wave, with a period dependent upon the inductance of the accelerometers. The remaining circuitry in the accelerometer channels is required to amplify and clip this voltage in order to define precisely the time of the end of this waveform. After this processing, the pulses which define the waveform termination in the two accelerometer channels are summed and used to fire the accelerometer multivibrator. Note that C1 is higher in value than C2. This prevents time overlap of the termination of the two accelerometer waveforms under any acceleration condition. A small amount of stray capacitance across the accelerometer coils results in the coupling of a fast positive going pulse at the beginning of the accelerometer waveform. After differentiation, this pulse results in a negative spike which fires the accelerometer multivibrator at the time of the commutator step, thus providing the accelerometer reference pulse. The output of the accelerometer multivibrator drives an Or gate in the same manner as the baro pulse.

### 2.3.4 Magnetometer channel

The sinusoidal output of the magnetometer is amplified by a feedback pair, Q14 and Q15. Two stages of feedback clipping, Q16 and Q17, result in a



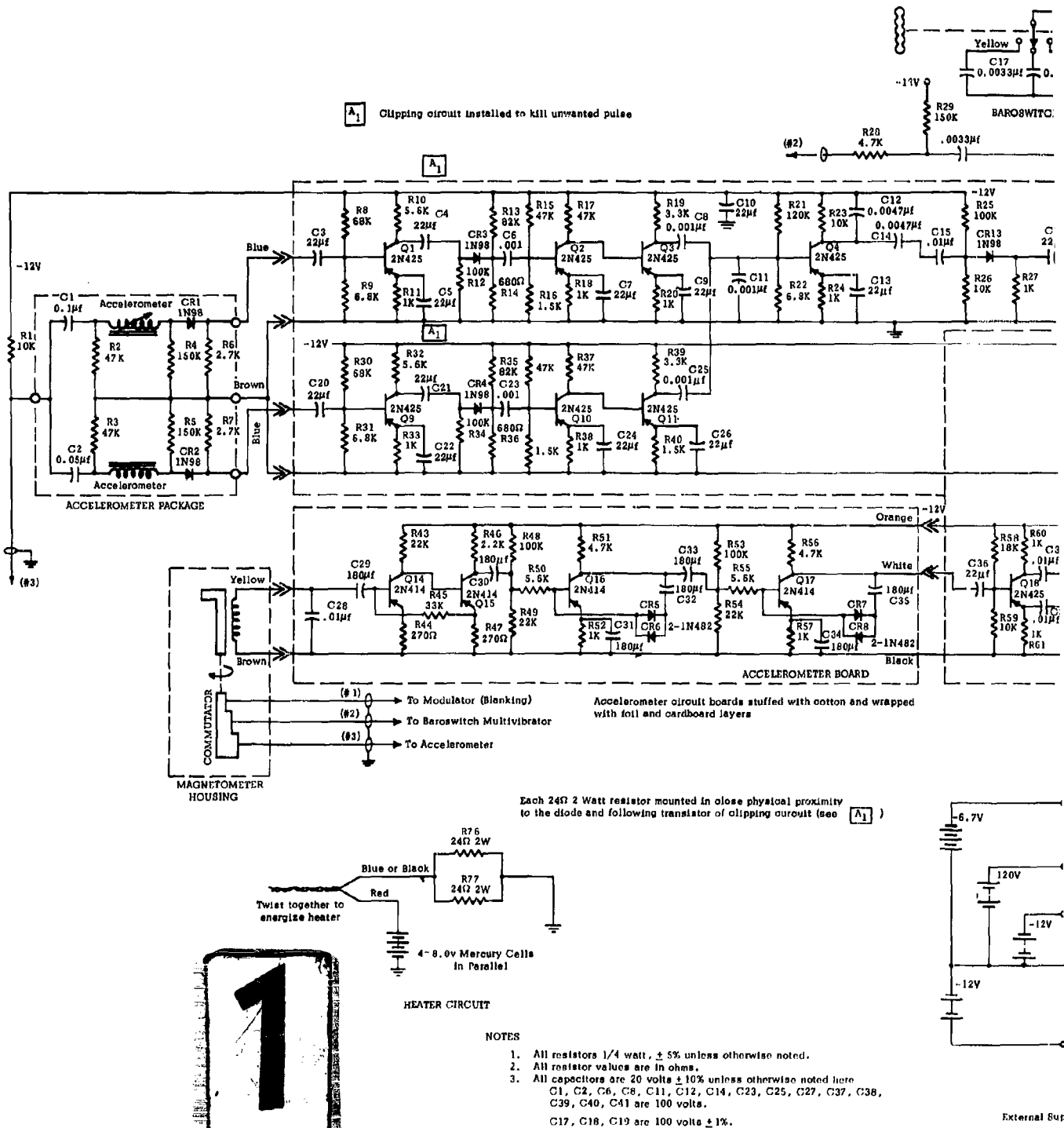


Figure 2.10 Schematic - Wind Shear

## 10 Schematic - Wind Shear Probe Instrument Package

substantially square wave output. This square wave drives phase splitter Q18, the output of which is differentiated. When a north crossing occurs, the collector output of Q18 is negativizing going, and the resultant negative pulse drives Q25 into conduction. The output of Q25 then fires the north multivibrator. A corresponding action occurs upon a south crossing, with Q19 firing the south multivibrator. The north and south multivibrator outputs drive Q22 through a diode Or gate. The output of this gate is shorted during the blanking time of the commutator in order to prevent transmission of azimuth information during the time that the remaining data channels are being read out.

## 2.4 Data Transmission

The pulses generated by the various functions of the wind shear probe amplitude modulate a radiosonde transmitter at 1680 mcs. This transmitter is coupled to a simple non-directive antenna system.

### 2.4.1 Modulator

The modulator transistor, Q23, is normally conducting heavily. Pulses from the various channels drive the base of Q23 positive, resulting in a negative output pulse of approximately 8 volts. These pulses are capacity coupled to the grid of the radiosonde oscillator, cutting it off during the pulse time.

### 2.4.2 Radiosonde oscillator

The radiosonde oscillator consists of a modified unit from the radiosonde AN/AMT-4. The modulator section is removed, and a connector added to the radio frequency output terminal to permit coupling to the Microdot coaxial cable antenna feed.

### 2.4.3 Antenna system

The output of the radiosonde is connected to a multicoupler, which divides power among four antennas. These antennas consist of quarter wave wires projecting from the wing surfaces, and operated with the metal wing serving as a ground plane. The feed lines to these dipoles are cut to provide 90° phase differences between adjacent dipoles, resulting in a circular radiation pattern.

## 2.5 Environmental Conditions

In the design of the probe, both temperature and altitude effects had to be carefully considered. Temperature proved the most critical problem - at the design altitude, temperature of the standard atmosphere is -67° F.

### 2.5.1 Temperature

Compatibility with this temperature environment was ensured by three means:

- 1) Proper component selection
- 2) Thermal insulation
- 3) Heating of critical parts

The transistors used in the wind shear probe (2N414 and 2N425) were selected especially for their excellent characteristics at low temperatures. Both types have been extensively tested at  $-60^{\circ}\text{C}$ , and their beta reduction from  $+25^{\circ}\text{C}$  to  $-60^{\circ}\text{C}$  is less than 30%. The coupling capacitors used in the various amplifier chains are tantalum types suitable for operation at  $-60^{\circ}\text{C}$ .

The nose cone of the wind shear probe is made of expanded polystyrene - an excellent insulating material. The battery power supply is placed in the nose cone to take advantage of this. The insulation plus internal heat developed in the batteries during discharge has proved sufficient to keep the batteries at operating temperature for 1.5 hours at  $-60^{\circ}$  to  $-80^{\circ}\text{C}$ .

The accelerometer packages are maintained at  $+92^{\circ}\text{F}$  by a resistance heating blanket operating from a 12-volt supply, and controlled by a thermostat.

#### 2.5.2 Altitude

Operation at the desired altitude (50,000 feet) posed relatively few problems. All voltages used in the probe are very low, so that no arcing is possible. The power supply chosen (mercury cells) is capable of operation in a vacuum and no volatile lubricants are used at any point.

#### 2.6 Power Supply

Power for the instrument package and parachute release mechanism are supplied from a battery pack of mercury cells. There are five separate supplies whose functions are listed below.

-12 volts	Measuring circuits and modulator supply
-12 volts	Accelerometer heater supply
-6.7 volts	Oscillator filament supply
+120 volts	Oscillator plate supply Parachute release supply
-8 volts	Accelerometer clipping circuit heater

#### 2.7 Parachute Mechanism

A modified AN/AMT-4A barometric pressure sensor is used to release the recovery parachute approximately 3000 feet above the ground. The modifications consist of opening all switch card contacts above the 3000' level and cutting the contact arm lift bar. The operation is as follows. Prior to launch, the switch

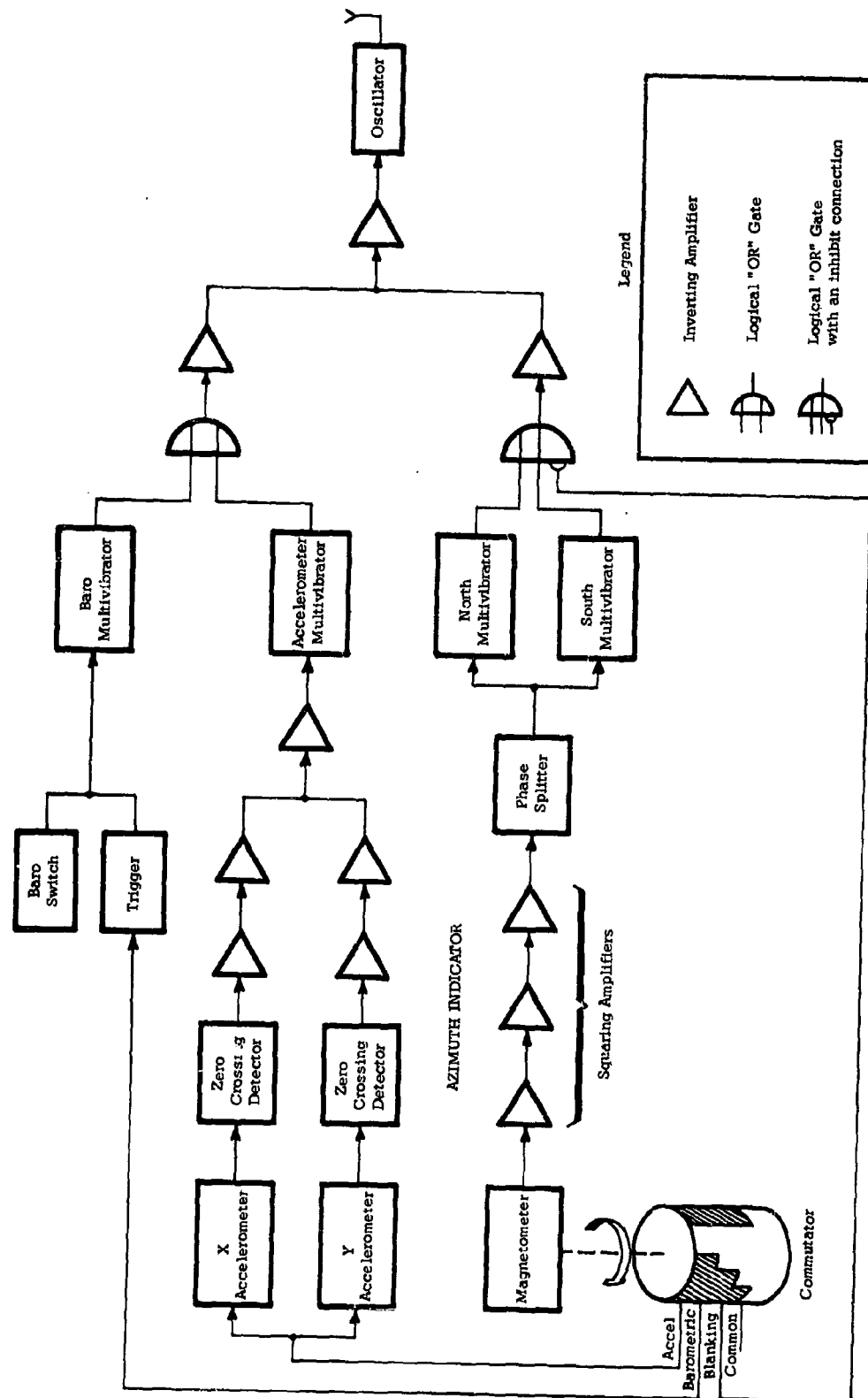


Figure 2.11 Wind Shear Probe Block Diagram

card contact is lifted off the card by the shortened lift bar. During ascent, the contact moves out along the lift bar and falls off after 10,000'. During descent, the contact moves back down the card until it contacts the 3000' level position. This completes the battery-operated relay circuit which releases the latching mechanism holding down the spring-loaded drogue. Upon release, the drogue is ejected from the probe dragging after it a 6' diameter mylar parachute.

## CHAPTER 3

### GROUND SUPPORT EQUIPMENT

#### 3.1 Rawin Receiver

In this section the simplified block diagram for the Rawin AN/GMD-1A set is shown for easy reference. No attempt will be made to describe its operation, since that is more adequately done in the Rawin instruction manual (Army Technical Manual TM11-271A).

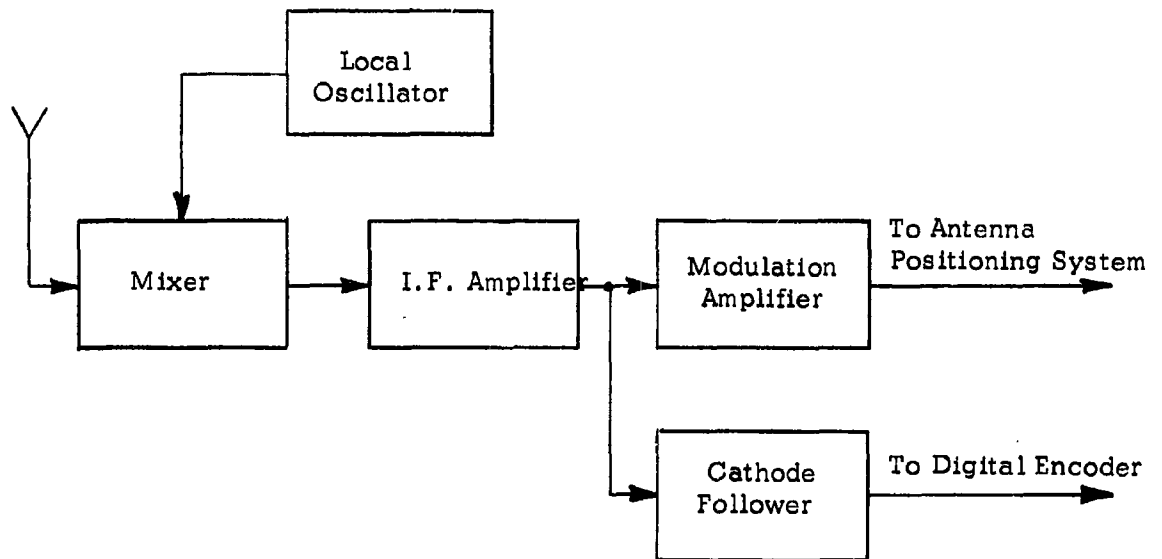


Figure 3.1 Simplified Block Diagram AN/GMD-1A

#### 3.2 Input Buffer

The Input Buffer serves three purposes:

- 1) Coupling the GMD-1A receiver to the encoder with proper impedances.
- 2) Inverting the pulse train from the GMD-1A receiver.
- 3) Removing transmission noise from the pulse train.

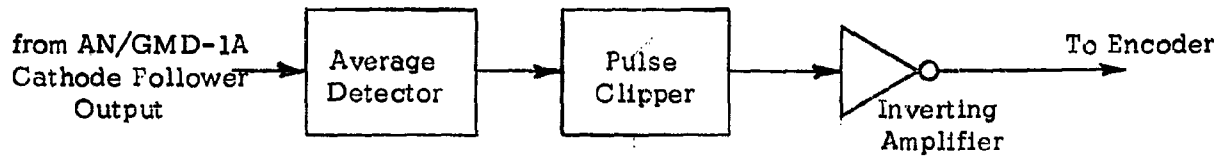


Figure 3.2 Input Buffer Block Diagram

Signals from the AN/GMD-1A receiver have their average level detected which allows the base line noise to be removed by the pulse clipper. An inverting amplifier transforms the pulse train to the proper polarity and adjusts the impedance level to that necessary to drive the encoder.

### 3.3 Ground Based Digital Encoder

#### 3.3.1 General

This equipment performs the function of identifying the components of the telemetered pulse train and routing them into the proper channels to be measured. Measurement is achieved, in the case of the barometric signal, by measuring the pulse duration. The remaining measurements are based on the time between related pulses.

In order to make a description of the logic more meaningful, consider the parameters to be measured and the method shown in Table 3.1.

Desired Measurement	Method of Measurement
1. Barometer	Baro pulse width
2. Wind acceleration (X direction)	Time from reference pulse to X accelerometer pulse ( $X_1$ to $X_{12}$ )
3. Wind acceleration (Y direction)	Time from reference pulse to Y accelerometer pulse ( $Y_1$ to $Y_{12}$ )
4. Azimuth sector	Azimuth pulse width determines north or south azimuth (N)
5. Azimuth angle	Time from reference pulse to the first azimuth pulse (C counter)
6. Number of measurements (frames)	Count the number of baro pulses ( $T_{1A}$ to $T_{12A}$ and $T_{1B}$ to $T_{12B}$ )

Table 3.1 Measurement Methods



First in the pulse train is the baro (barometric) pulse, from which two pieces of information are gleaned: (1) position of the baro switch contact and (2) the number of frames of data. The baro pulse is used to count frame number for two reasons:

- 1) the baro pulse is present in every frame
- 2) the baro pulse width is totally different from all other pulses in the system.

In the discussion that follows, it will be necessary to refer to Figure 3.3 and the encoder block diagram. In Figure 3.3, the following definitions are used:

- 1) multivibrator - commonly called delay multivibrator - the pulse length is determined by the internal circuit and is fixed.
- 2) flip-flop - a circuit with two stable states. Two types are used in this system.
  - a. a flip-flop with a "C" (count) input will change state each time a pulse is presented to the "C" input.
  - b. a flip-flop without a "C" input will remain in its last state until triggered by a pulse on the "s" (set) input or reset by a pulse on the "R" input.

### 3.3.2 Barometer encoding

The input pulse train has, for its first pulse, the baro pulse which triggers three useful events in the circuits attached to point 1 of Figure 3.3. Reading from the top left of Figure 3.3 downward, these events are: triggering of the  $150\mu$  sec multivibrator; triggering of the  $160\mu$  sec multivibrator; and triggering of the  $5\mu$  sec multivibrator. The baro pulse also triggers two non-useful events, which are not allowed to proceed. These events are: triggering the  $10\mu$  sec multivibrator between points 1 and 13 and triggering the AND gate between points 1 and 20. In both cases the gates are not permissive and the pulse can propagate no further.

Returning to the useful events, consider the components connected between points 1 and 4; this group of components make up the baro pulse recognition circuit. Baro pulse has four possible lengths; 175, 225, 275 or 325 microseconds. Pulses of shorter duration will be rejected. See Figure 3.4 for timing diagram showing recognition of

- 1) baro pulse
- 2) non-baro pulse

Figure 3.4a shows recognition of a baro pulse with minimum width of  $175\mu$  seconds. Line 4 (point 4 in Figure 3.3) goes negative when lines 2 and 3 negative. Figure 3.4b shows recognition of a non-baro pulse. Lines 2 and 3 are simultaneously

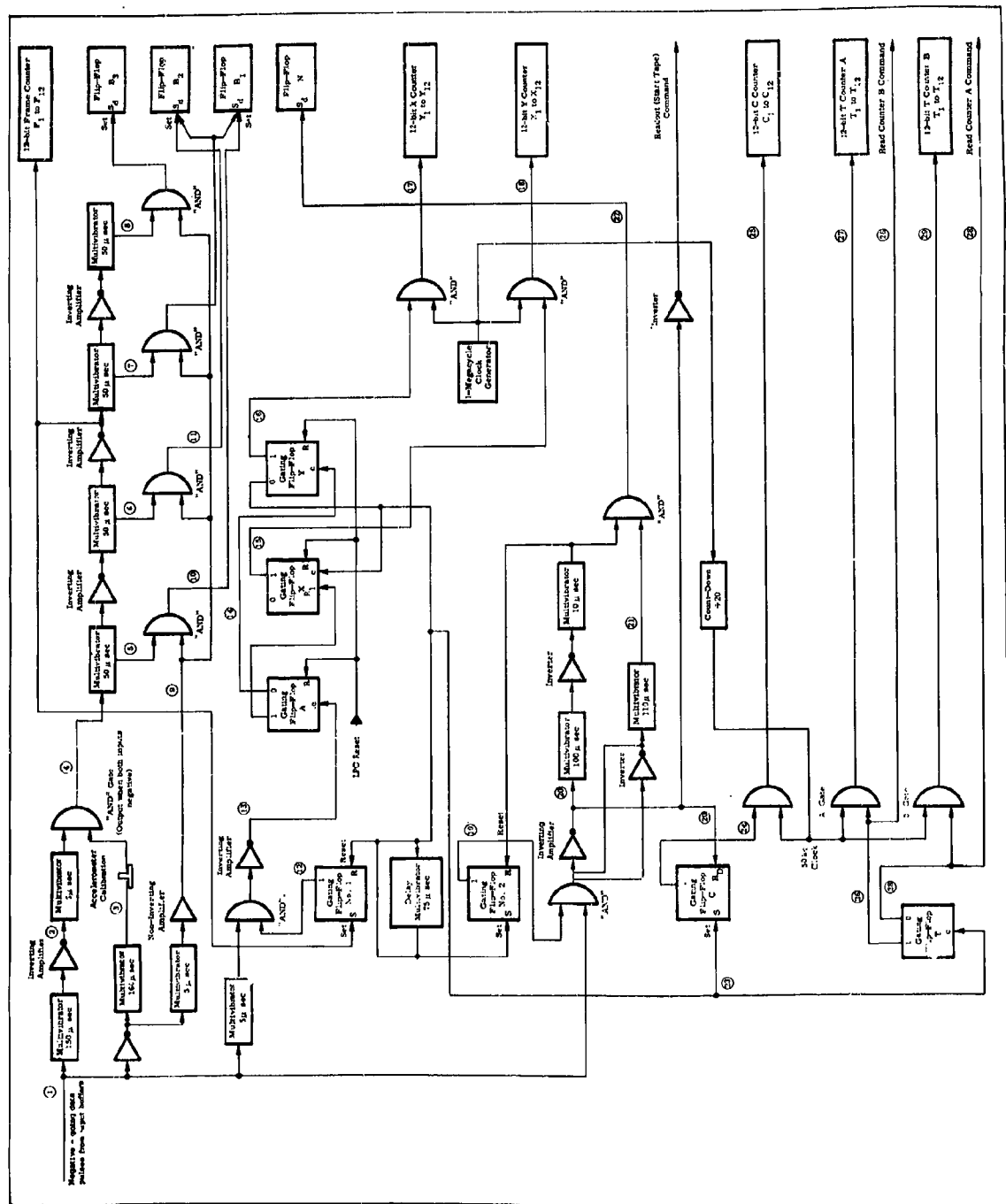
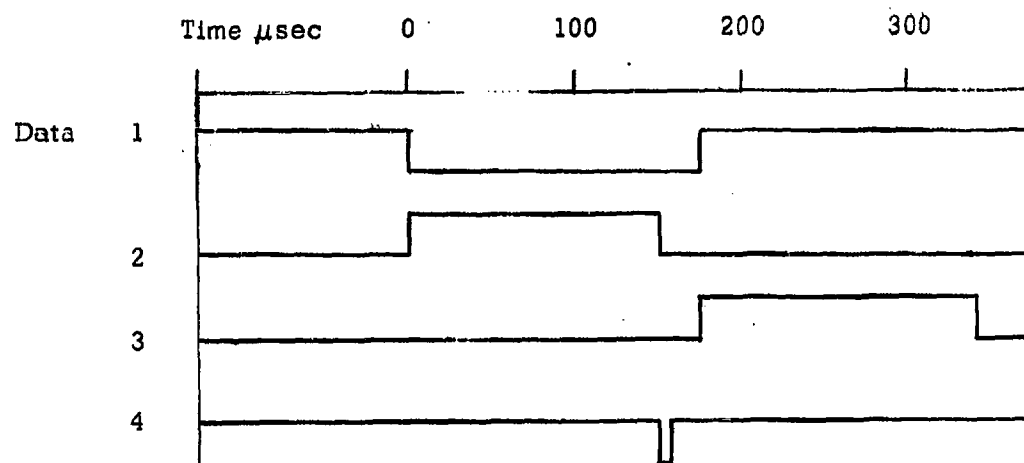
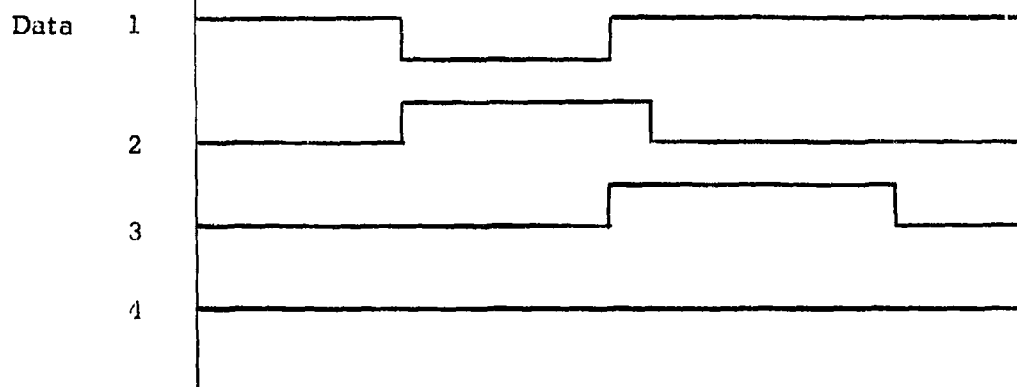


**Figure 3.3 Encoder Block Diagram**



a) Recognition of a Baro Pulse



b) Recognition of a Non-Baro Pulse

Figure 3.4 Timing Diagram - Baro Pulse Recognition

negative, but the  $5\mu$  second multivibrator following point 2 goes negative only when point 2 goes negative and then stays negative for only  $5\mu$  seconds. Therefore line 4 shows no pulse or recognition of a non-baro pulse.

Once the baro pulse is recognized at point 4, it is sent to the frame counter and to a logic network which determines the width of the pulse. Timing of the pulse width gates is shown in Figure 3.5, Lines 5, 6, 7 and 8. These gates are permissive when point 4 and any one of points 5, 6, 7 and 8 are negative at the same time. Two examples are illustrated in Figure 3.5. One starts at the left and indicates a baro pulse of  $225\mu$  second width; coincidence occurs with lines 4 and 6; the result being indicated on line 11. The second example at the right indicates a baro pulse of  $175\mu$  second pulse width; coincidence occurs with line 4 and line 5, the result is shown on line 10. Outputs of the AND gates connected to points 5, 6, 7 and 8 drive three flip-flops -  $B_1$ ,  $B_2$ , and  $B_3$ ; Table 3.2 shows the coding format of this register.

Baroswitch Contacts Closed	Pulse width	$B_1$	$B_2$	$B_3$
None	$175\mu$ sec	1	0	0
Humidity	$225\mu$ sec	0	1	0
Low Reference	$275\mu$ sec	1	1	0
High Reference	$325\mu$ sec	0	0	1

Table 3.2 Coding Format Baropulse

### 3.3.3 Accelerometer encoding

After the baro pulse come the reference X and Y accelerometer pulses: the last three are each 20 microseconds long. Measurement of acceleration magnitude is made by measuring the time between arrivals of the reference pulse and the subject accelerometer pulse.

When the baro pulse is recognized at point 4 (Figure 3.3), the resulting pulse "sets" Gating Flip-Flop No. 1 whose output (point 12) makes the Accelerometer Input and Gate permissive. The reference pulse triggers a  $5\mu$  second multivibrator (Figure 3.3, four rows from top); the output of the associated AND gate and inverting amplifier (point 13) triggers Gating Flip Flop A. The "1" output of A triggers Flip-Flop X whose output (point 15) makes the X counter gate permissive and allows 1 megacycle pulses to be counted in the X register. The "0" output of A triggers Flip-Flop Y, whose output (point 16) makes the Y counter gate permissive and allows 1 megacycle pulses to be counted in the Y register.

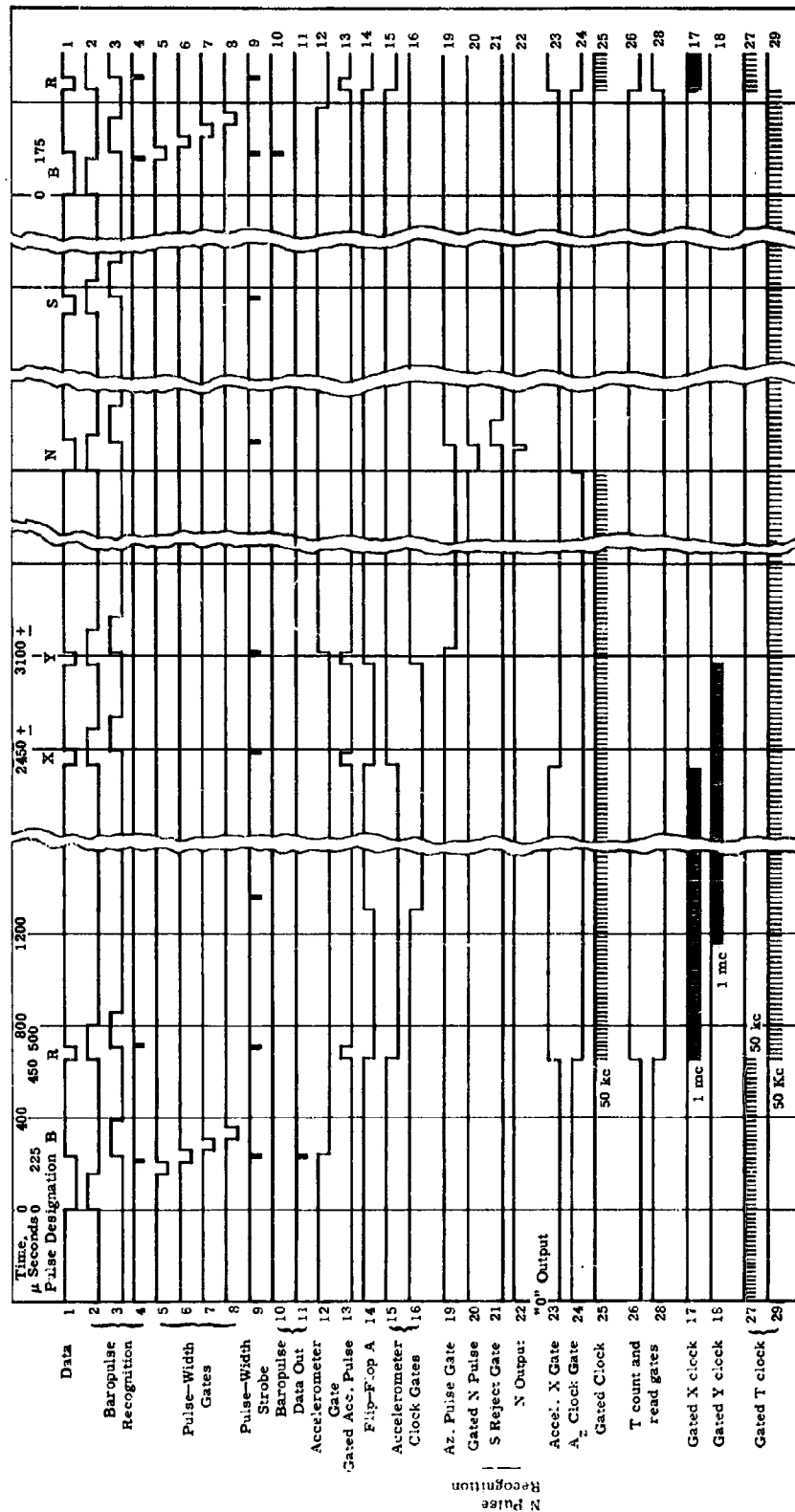


Figure 3.5 Wind Shear Probe - Digital Encoder - Tuning of Waveforms

Next in the pulse train is the X accelerometer pulse which goes through the accelerometer input gate in the same manner as did the reference pulse. The  $5\mu$  second multivibrator resets Gating Flip Flop A which, in turn, resets Gating Flip Flop X. The output line of this Flip Flop (point 15) "closes" the X accelerometer gate and stops the X counter.

Stopping the Y counter is similar to that used for the X except the Y Gating Flip Flop is the one which is reset.

#### 3.3.4 Azimuth encoding

Azimuth information is coded by recognizing a north or south magnetic field crossing and measuring the time from the appearance of the reference pulse to the appearance of the north or south pulse, whichever occurs first. The pulse width characteristics are as follows:

- 1) North crossing pulse - 125 microseconds
- 2) South crossing pulse - 75 microseconds

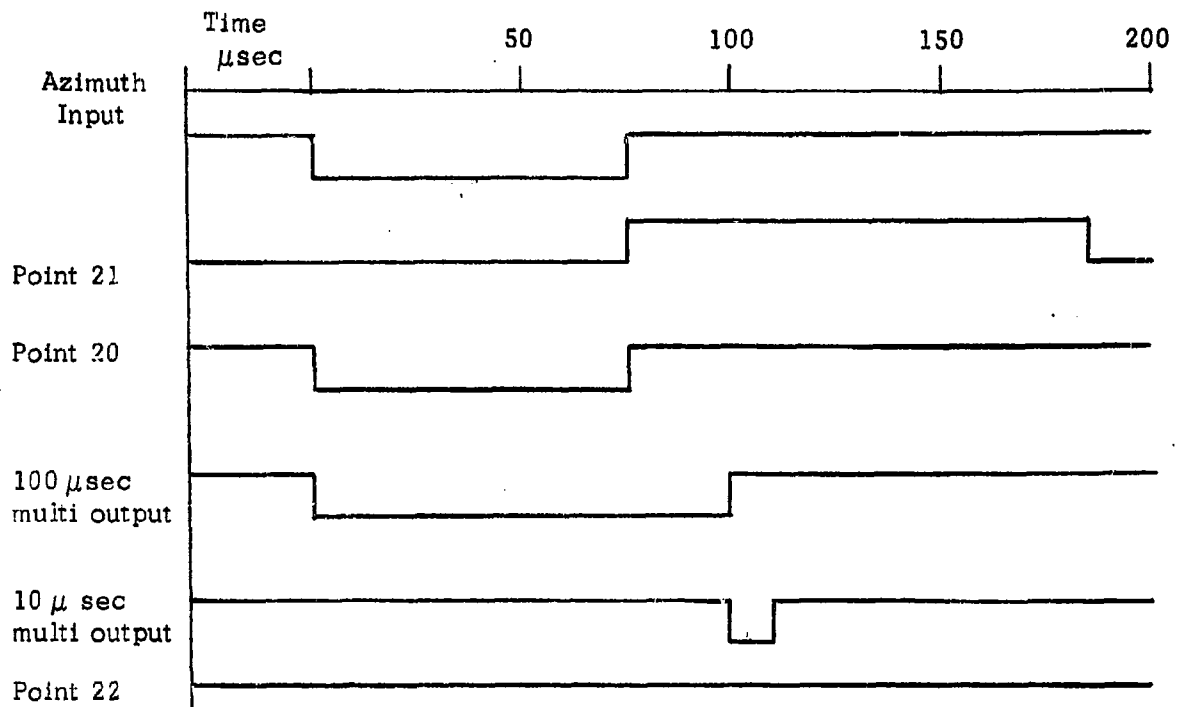
The azimuth pulse recognition circuit starts at the AND gate connected between points 1 (see Figure 3.3) and 20. This gate is made permissive by receipt of the Y accelerometer pulse. An azimuth pulse is received, passed through the AND gate and an inverting amplifier, and triggers a  $110\mu$  second delay multivibrator with the trailing edge of the pulse, (point 21). This makes the AND gate which follows the multivibrator permissive for  $110\mu$  seconds. At the same time, the output of the inverting amplifier is re-inverted (point 20) and triggers a  $100\mu$  second delay multivibrator which, in turn, triggers a  $10\mu$  second delay multivibrator. If the output of this delay multivibrator is in coincidence with point 21, the AND gate produces an output (point 22) which will trigger the "N" Flip Flop. This indicates that a North crossing has been recognized. Figure 3.6 shows the timing diagram for recognition of both North and South crossings.

Azimuth magnitude is measured from the time of receipt of the reference pulse to the time of receipt of the first azimuth pulse. At the same time that the reference pulse is starting the accelerometer counters, it is sent to point 23 where it triggers a Gating Flip Flop whose output makes an AND gate (point 24) permissive. This starts the azimuth counter counting 50 kilocycle pulses. When the azimuth pulse arrives, it

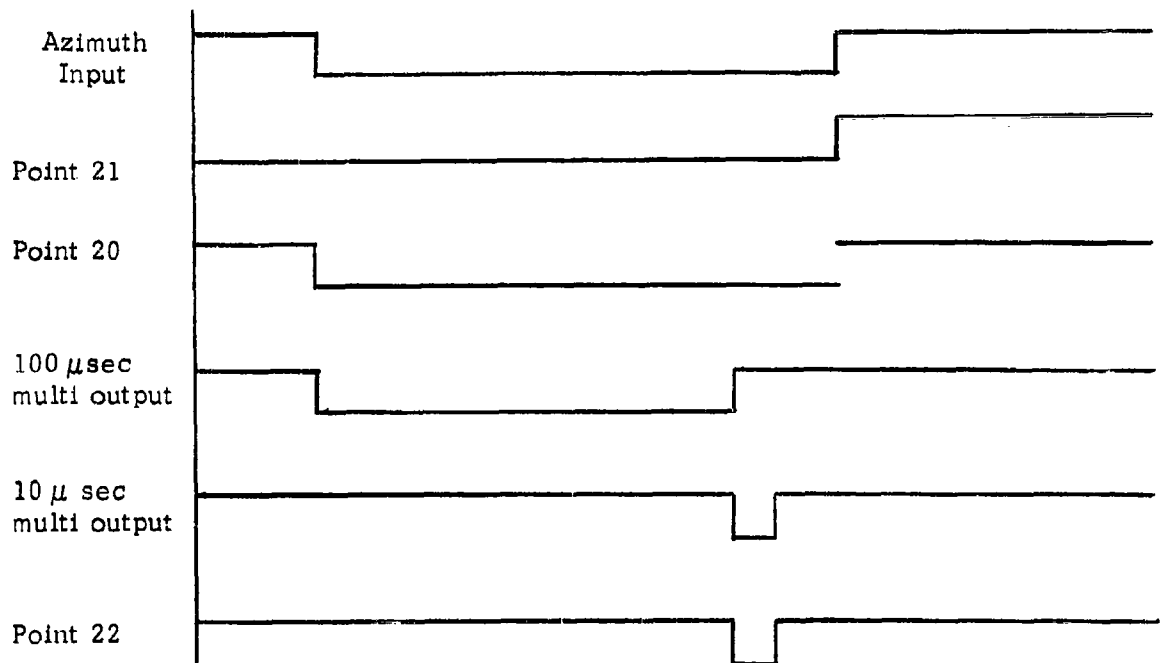
- a. stops the azimuth counter ("C" counter).
- b. starts the tape readout cycle (point 20).

#### 3.3.5 Vertical velocity encoder

It is desired to determine the speed of the air log rotation. This is achieved by counting the time interval between reference pulses since each reference pulse is equivalent to one rotation of the air log. In order that no data be lost, two counters ("I" counters) are provided which count on alternate cycles.



a) Recognition of South Crossing



b) Recognition of a North Crossing

Figure 3.6 Timing Diagram - Azimuth Recognition

The first reference pulse enters the velocity encoder at point 23 and triggers Gating Flip Flop "T". The "1" output (point 28) makes the AND gate connected to that point permissive; it also sends a "read counter A" command. The second reference pulse causes the Gating Flip Flop to change state. The "1" output disables the counter B gate. The "0" output sends a "read counter B" command and makes the "A" counter gate permissive. The third reference pulse repeats the cycle.

### 3.4 Read-Out Matrices

The purpose of the read-out matrix is to transfer information stored in the encoder to the tape recorder. If "analog recording" techniques were used, the matrix would be unnecessary since each information "bit" would be recorded as it occurred. Analog recording, after encoding, unnecessarily complicates data correlation and processing.

The recording technique used is digital, which requires simultaneous presentation of seven bits of information to the seven channels of the tape recorder. The recorder then indexes to the next position and records seven more bits of information. This process continues until one frame (16-1/2 lines) is complete. (Figure 3.7 shows the tape format.)

A block diagram of the "Readout Matrix" is shown in Figure 3.8 and a timing diagram for this system is shown in Figure 3.9. It will be necessary to refer to these two figures during the ensuing discussion.

The readout cycle begins when a start readout pulse (1) is received from the encoder. This pulse starts the tape recorder (3) and opens the first gate in the tape and read clock circuits (4). The first tape clock pulse (5) after the gate (4) is enabled triggers a flip flop (7) and enables the read clock gate. The first read clock pulse following the enabling of the readout gate (7), gives the gated read pulse (8) and enables the tape clock gate which permits the next tape clock pulse (5) to be passed (10). Each of these gates is reset by the clock pulse which is passed through it, and the procedure repeats itself.

The gated read clock provides timing pulses to the read line gates which determine the line readout sequence. This sequence is shown in the timing diagram of Figure 3.9.

Thirty microseconds after each gated read clock pulse, a gated tape pulse appears. This pulse enables the tape read driver gates and resets the readout flip flops. During the gated tape clock pulse, the driver flip flops transmit their information to the tape recorder.



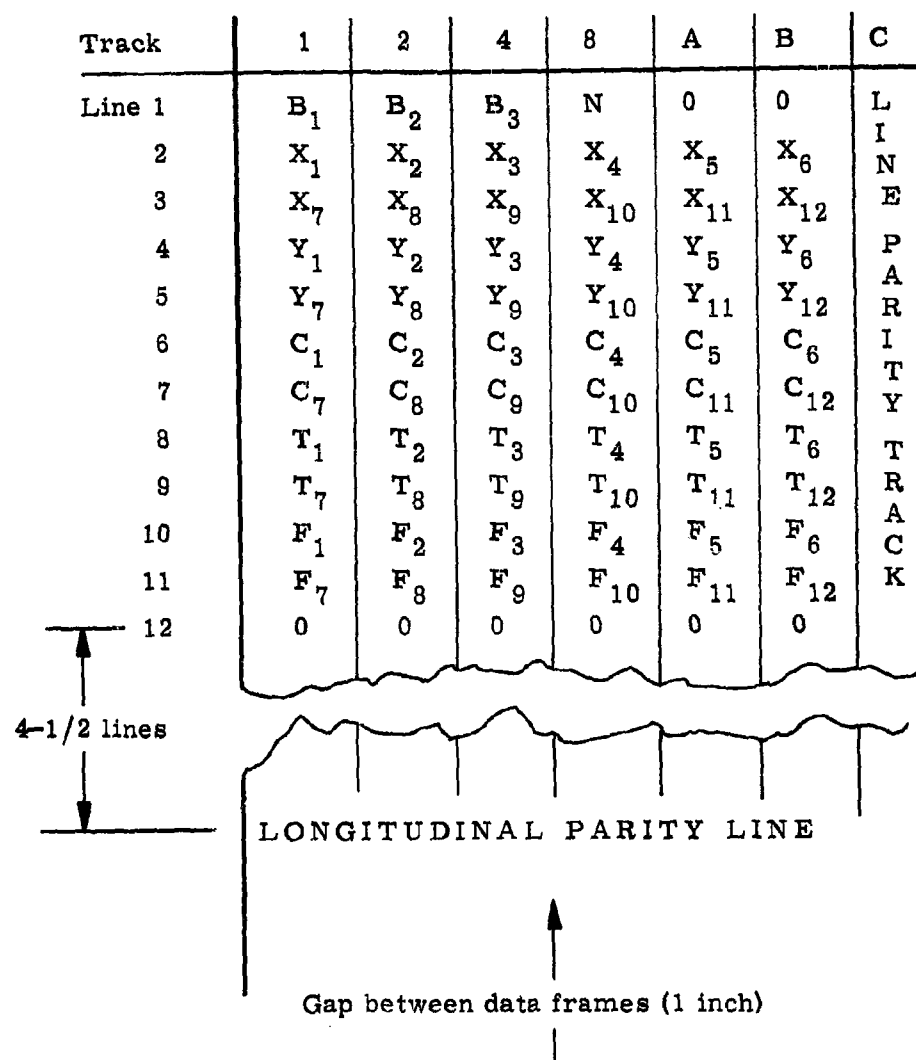


Figure 3.7 Wind Shear Probe - IBM Digital Data Tape Format

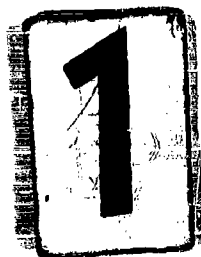
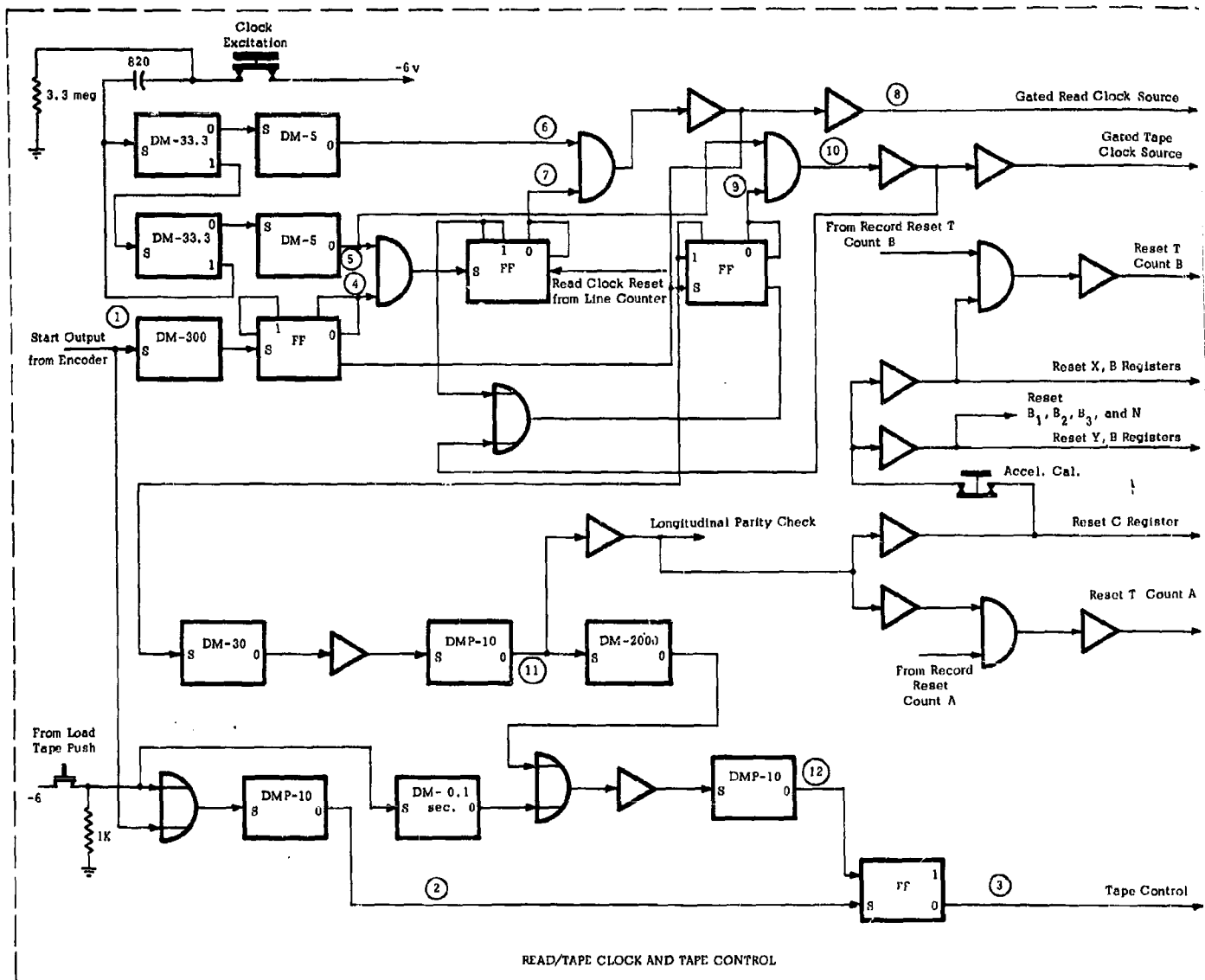


Figure 3.8 Readout

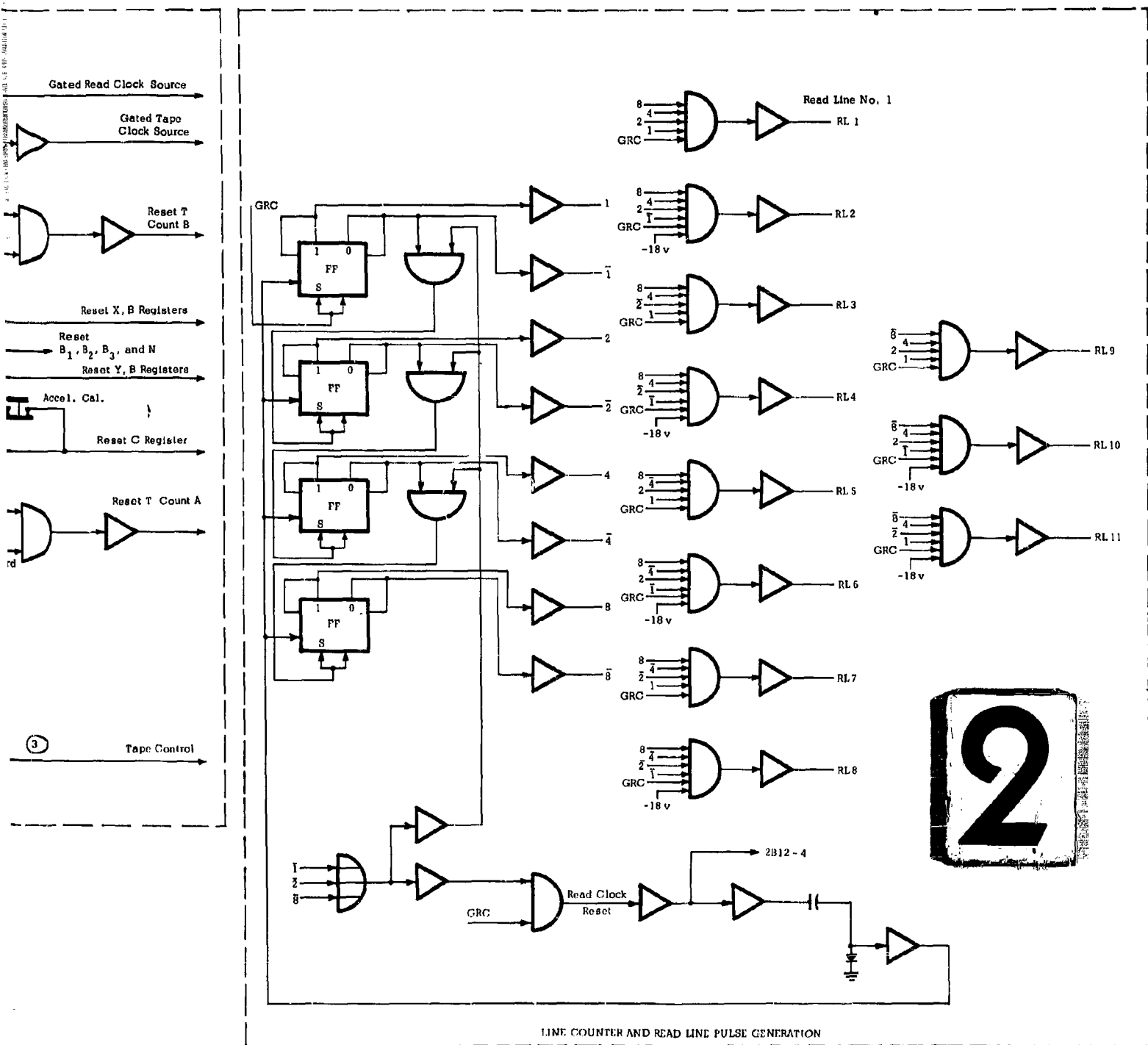


Figure 3.8 Readout Matrix

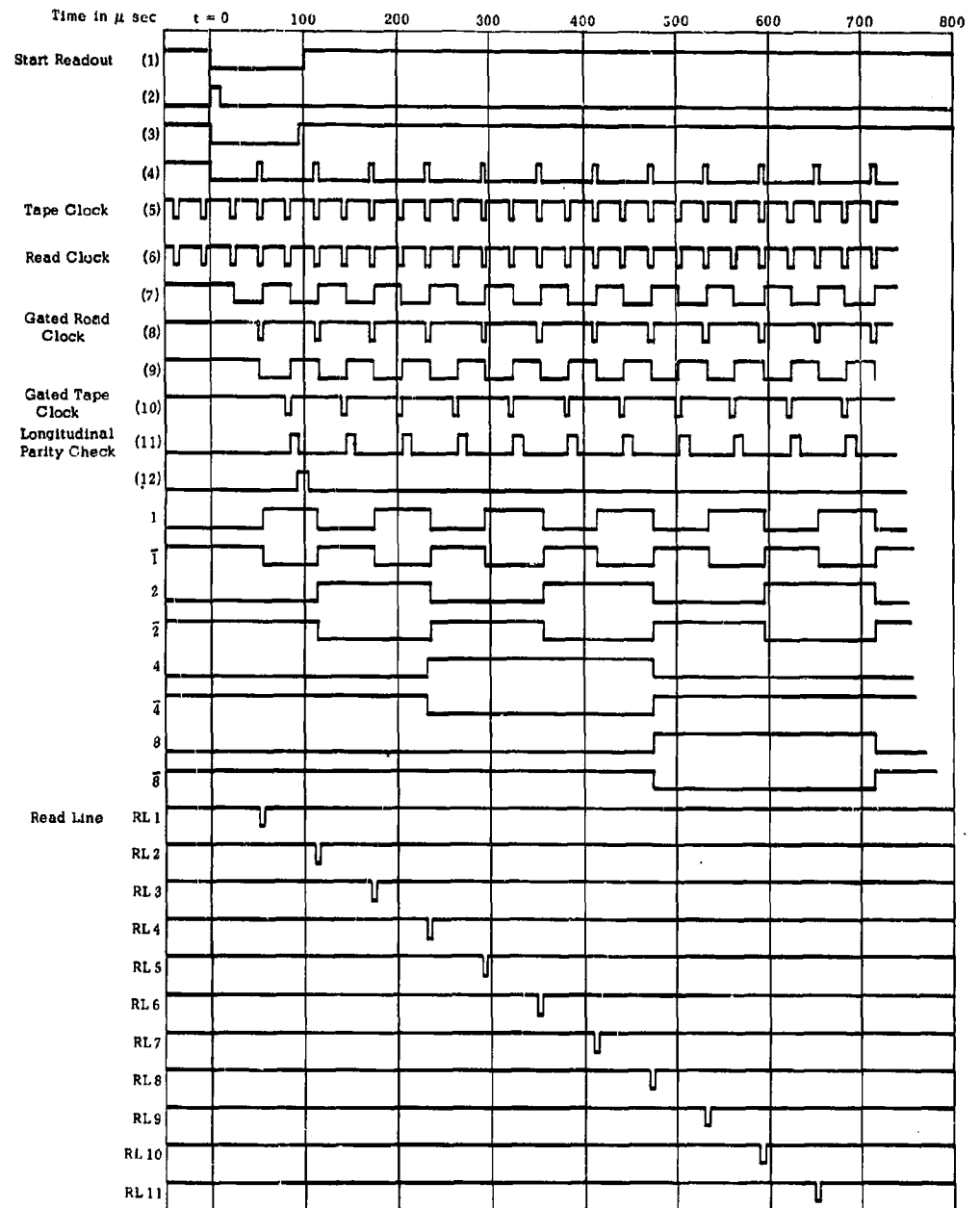


Figure 3.9 Timing Diagram Readout Matrix

### 3.5 Parity Generator

The IBM 704 computer format requires an odd number of "ones" in each line. Since the information channels are not dependent on one another, it is not possible to design the encoding logic to give us an odd number of "ones" in each line; therefore it becomes necessary to generate a signal which will give the recording an odd number of "ones" on each line. The parity generator serves this purpose.

The parity generator is designed to examine the outputs of Channels 1, 2, 4, 8, A and B and determine the number of "ones" in each line. If there are an even number of "ones", the parity generator will generate a pulse which will add an extra "one" to the line.

Inputs to the parity generator are from the read line flip flops. "Ones" are fed in on lines marked 1, 2, 4, 8, A and B; "Zeros" are fed in on lines 1, 2, 4, 8, A and B.

### 3.6 The Ground Logic Simulator

The purpose of the ground logic simulator is to provide a test circuit which can be used to make a final check of the ground logic system.

The function of this circuit is to generate five pulses which simulate the ground receiver output in pulse width, pulse spacing and repetition rate. By feeding this signal into the input of the ground logic and comparing the output information with it, it can be determined if the ground logic system is functioning properly.

These five pulses represent the baro pulse, the reference pulse, the two accelerometers, and the north azimuth crossing pulse.

The pulse repetition rate is determined by the free running multivibrator which has a repetition rate of approximately 36 cycles per second. The output of the multivibrator, a negative going sweep, is coupled to a buffer amplifier. The output of this buffer feeds five individual amplifiers, one for each output pulse. These amplifiers are cut off until the sweep from the multivibrator drives them to saturation. The switching point, and therefore the time delay between pulses, is determined by the bias adjustment.

Each amplifier is coupled to a Schmitt trigger which fires when the amplifier is switched. The output of the Schmitt trigger is differentiated and fed into a delay multivibrator. In the baro pulse channel, a delay multivibrator produces the proper baro pulse width, which is fixed at  $225\mu$  sec. The differentiated Schmitt trigger outputs of reference, accelerometer one, and accelerometer two

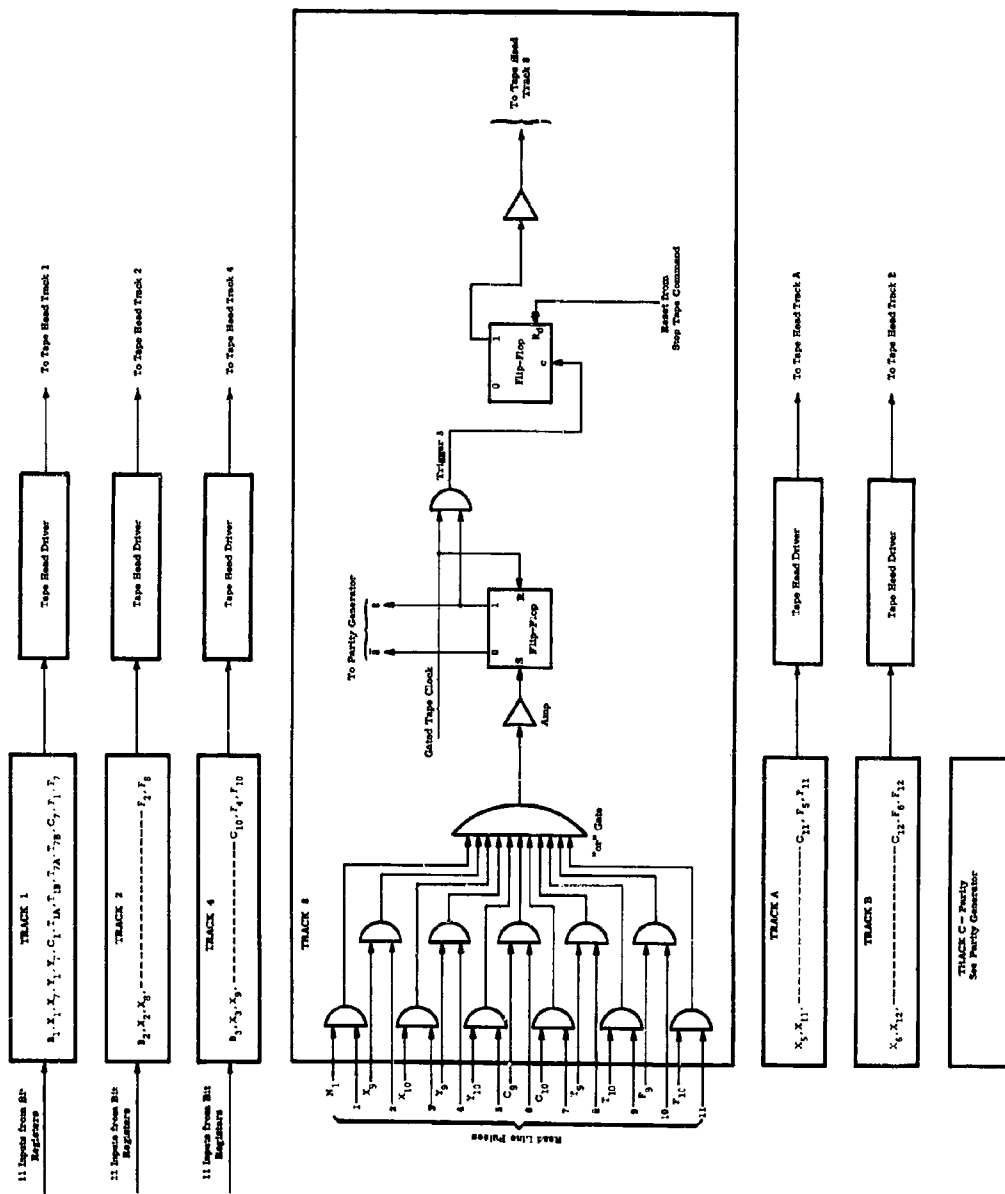


Figure 3.10 Read Line Gates

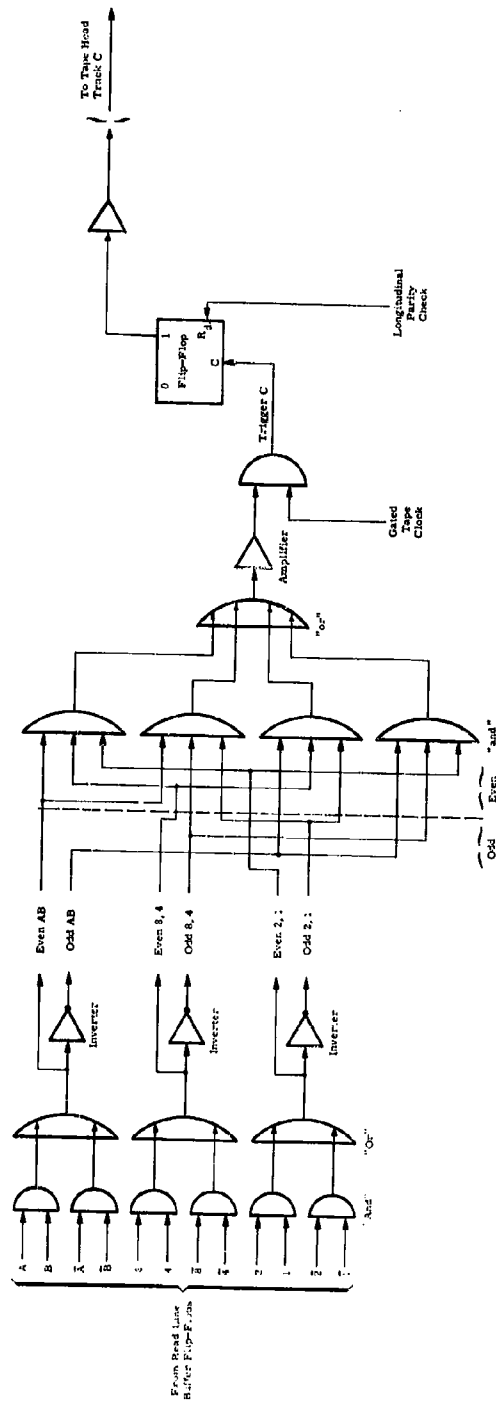


Figure 3.11 Parity Generator

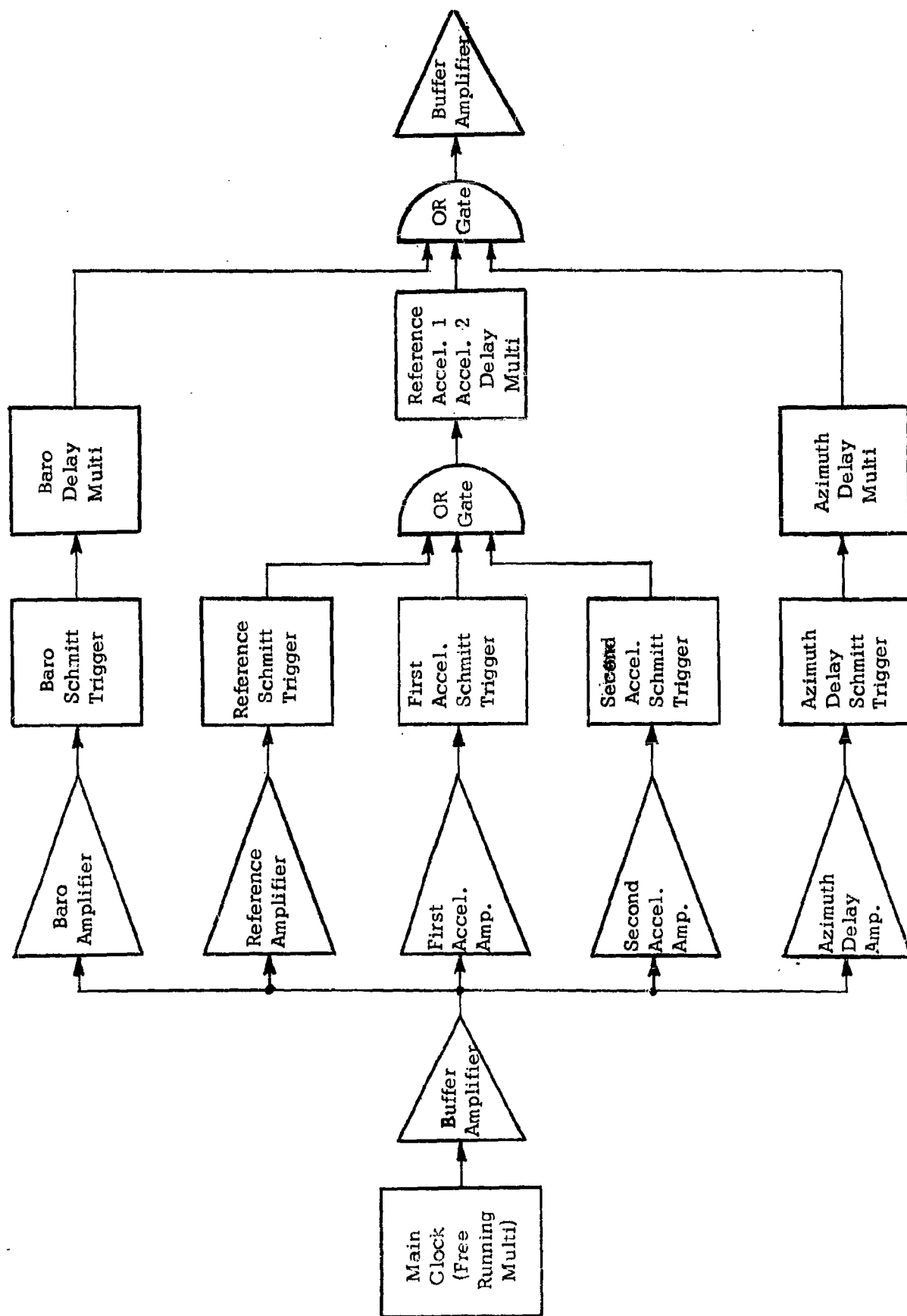


Figure 3.12 Block Diagram of Wind Shear for Gnd-1 Receiver



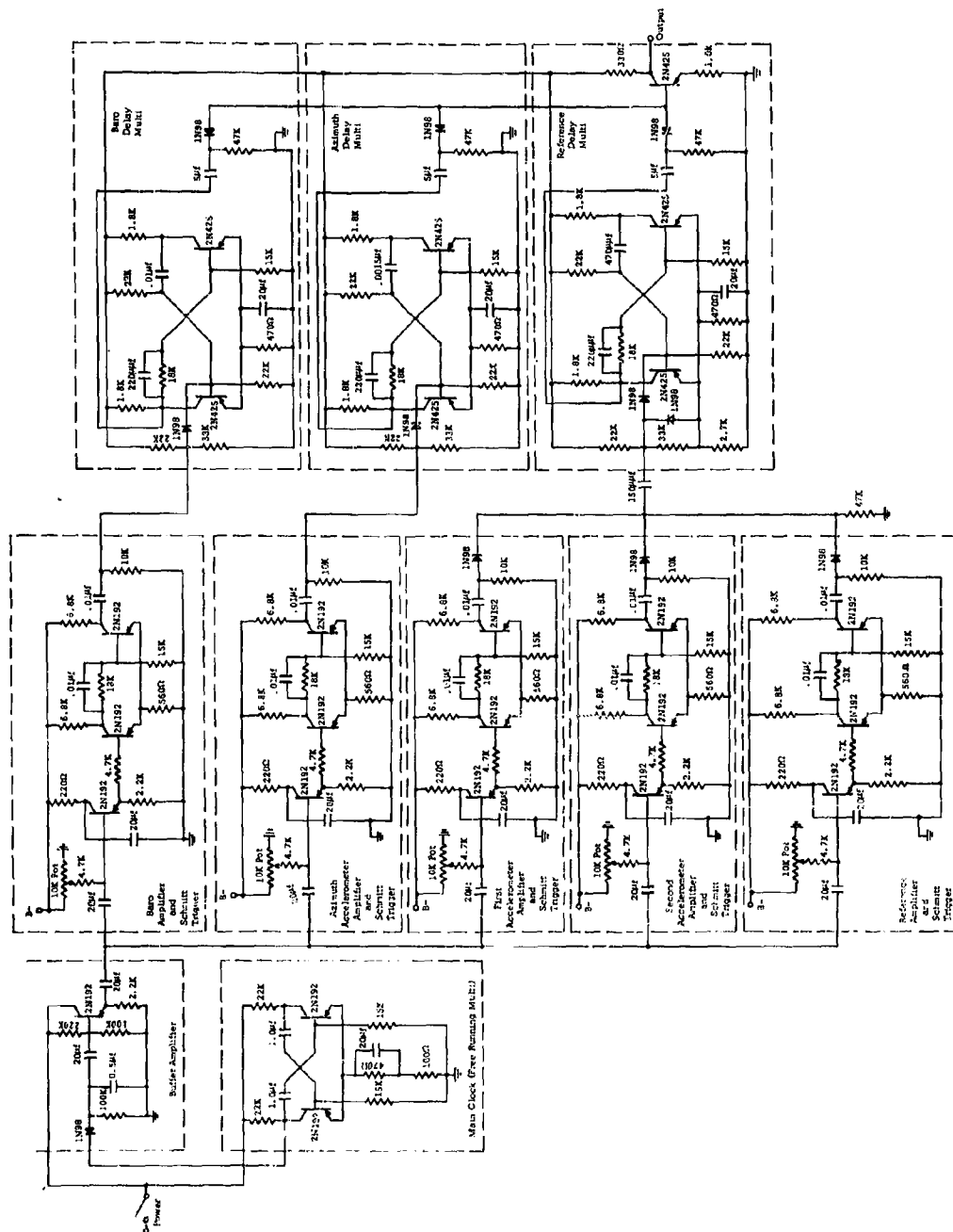


Figure 3.13 Wind Shear Simulator for Gnd-1 Receiver to Data Reduction System

channels are coupled to a diode Or gate which drives a 20 microsecond delay multivibrator. The output of the north crossing Schmitt trigger is also coupled to a delay multivibrator which generates a 175 microsecond pulse.

The outputs of the three delay multivibrators are combined into a diode Or gate which feeds an output buffer amplifier.

The simulator schematic is shown in Figure 3.13.

## CHAPTER 4

### TESTING

Testing of the wind shear probe in the laboratory consisted basically of operational checks with a cold environment. Field test of one instrumented probe was unsuccessful.

#### 4.1 Laboratory Testing

Extensive unit and system testing of the probe and ground readout system was accomplished in the URI laboratory. After unit testing of each module, the probe R.F. output was connected to the GMD-1 receiver through an attenuator. The attenuator was set to a level corresponding to the estimated free space loss from the probe antenna to the GMD-1 receiver terminals, with the probe at a slant range of 70,000 feet. The entire system, including the tape recorder, was then checked by noting the readout on the digital tape for known probe inputs. During these tests, the probe air screw was driven by means of compressed air. Operation over the range of anticipated air screw rotation rates was checked and found to be satisfactory.

Final testing of the probe system consisted of a test setup the same as described above except that the probe was suspended in an insulated container which was lowered in temperature to  $-80^{\circ}$  F. Under these conditions, proper operation of all instrumentation was noted for a period of 1.5 hours. Since the total anticipated flight time of the probe is less than .75 hour, it appears that the test was conservative.

#### 4.2 Field Testing

Field tests were conducted at White Sands Missile Range, New Mexico. After considerable difficulties with range scheduling, as well as balloons and release mechanisms, a fully instrumented probe was launched. Radar tracks of the probe showed that the release mechanism did not operate properly, since an altitude of 53,000 feet was achieved, and the mechanism was designed to release at 40,000 feet. In addition, the GMD-1 receiver failed to receive telemetry signals from the probe radiosonde.

## CHAPTER 5

### CONCLUSIONS

The wind shear probe appears to be a basically sound method for the measurement of wind shear as a function of altitude. The probe requires further field evaluation, following a program of thorough laboratory testing to increase the probability of success. Further coordination in field testing is needed, particularly with regard to frequency acquisition of the probe transmitter by the GMD-1 receiver before launch.

# DISTRIBUTION LIST

ARDC Liaison Office U. S. Army Signal Research and Development Laboratory Fort Monmouth, New Jersey ATTN: SIGRA/SL-LNA	1	Commanding Officer U. S. Army Signal Research and Development Laboratory Fort Monmouth, New Jersey ATTN: SIGRA/SL-SMA	8
U. S. Navy Electronics Liaison Office U. S. Army Signal Research and Development Laboratory Fort Monmouth, New Jersey ATTN: SIGRA/SL-LNS	1	OASD (R&E) The Pentagon Washington 25, D. C. ATTN: Technical Library	1
USCONARC Liaison Office U. S. Army Signal Research and Development Laboratory Fort Monmouth, New Jersey ATTN: SIGRA/SL-LNP	1	Chief of Research and Development OCS, Dept. of the Army Washington 25, D. C.	1
Commanding Officer U. S. Army Signal Research and Development Laboratory Fort Monmouth, New Jersey ATTN: SIGRA/SL-DR	1	Chief Signal Officer Department of the Army Washington 25, D. C. ATTN: SIGRD	1
Commanding Officer U. S. Army Signal Research and Development Laboratory Fort Monmouth, New Jersey ATTN: SIGRA/SL-ADT	1	Director U. S. Naval Research Laboratory Washington 25, D. C. ATTN: Code 2027	1
Commanding Officer U. S. Army Signal Research and Development Laboratory Fort Monmouth, New Jersey ATTN: SIGRA/SL-ADJ (Responsible File and Record Unit)	1	Commanding Officer and Director U. S. Navy Electronics Laboratory San Diego 52, California	1
Commanding Officer U. S. Army Signal Research and Development Laboratory Fort Monmouth, New Jersey ATTN: SIGRA/SL-TNR	8	Commander Air Force Command & Control Development Division Air Research and Development Command USAF ATTN: CROTL Laurence Hanscom Field Bedford, Massachusetts	1
		Commanding General U. S. Army Electronic Proving Ground Fort Huachuca, Arizona	1
		NASA, Langley Research Center ATTN: Mr. H. Tolefson, Atmospheric Inputs Section Dynamic Loads Div., Langley Field, Virginia	1

# DISTRIBUTION LIST (Cont.)

Commander	10	Chief of Naval Operations (OP07)	1
Armed Services Technical Information Agency		U. S. Navy Department	
Arlington Hall Station		Washington 25, D. C.	
Arlington 12, Virginia		Office of Naval Research	1
ATTN: TIPDR		U. S. Navy Department	
		Washington 25, D. C.	
Chairman		U. S. Naval Research Laboratory	1
U. S. Army Chemical Corps	1	Code 7110	
Meteorological Committee		Washington 25, D. C.	
Ft. Detrick, Frederick, Maryland			
Chief	1	Director	1
Meteorology Division		U. S. Naval Weather Service	
U. S. Army Chemical Corps		U. S. Naval Station	
Proving Ground		Washington 25, D. C.	
Dugway Proving Ground, UTAH		Officer-in-Charge	1
Chemical Research & Development Laboratories	1	U. S. Naval Weather Research Facility	
Technical Library		U. S. Naval Air Station, Bldg. R48	
Army Chemical Center		Norfolk, Virginia	
Edgewood, Maryland		Office of the Chief of Ordnance	1
Director	1	Department of the Army	
Atmospheric Sciences Programs		Washington 25, D. C.	
National Science Foundation		Chief, Research Laboratory	2
Washington 25, D. C.		R&D Operations	
Director	1	Army Ballistic Missile Agency	
Bureau of Research & Development		Redstone Arsenal, Alabama	
Federal Aviation Agency		ATTN: Mr. Reisig	
Washington 25, D. C.		Commanding Officer	1
Chief	1	U. S. Army Signal Missile Support Agency	
Bureau of Naval Weapons (FAME)		White Sands Missile Range	
U. S. Navy Department		New Mexico	
Washington 25, D. C.		ATTN: Missile Geophysics Division	
Officer-in-Charge	1	Chief, West Coast Office	1
Meteorological Curriculum		U. S. Army Research & Development Laboratory	
U. S. Naval Post Graduate School		75 South Grand Ave., Bldg. 6	
Monterey, California		Pasadena 2, California	

# DISTRIBUTION LIST (Cont.)

The University of Texas Electrical Engineering Research Laboratory Austin, Texas ATTN: Mr. Gerhardt	1	U. S. Naval Air Missile Test Center Meteorological Division Point Mugu, California ATTN: Mr. Masterson	1
Office of Technical Services Department of Commerce Washington 25, D. C.	1	Director Federal Aviation Agency Pomona, New Jersey ATTN: Mr. Hilsenrod	1
American Meteorological Society Abstracts and Bibliography P. O. Box 1736 ATTN: Mr. Malcolm Rigby Washington 25, D. C.	1	Signal Corps Liaison Office, MIT, 77 Massachusetts Avenue Building 20C-116 Cambridge 39, Massachusetts ATTN: Mr. A. Bedrosian	1
Library National Bureau of Standards Washington 25, D. C.	1	Library U. S. Weather Bureau Washington 25, D. C.	1
Department of Meteorology University of Wisconsin Madison, Wisconsin	1	Meteorology Department Pennsylvania State College State College, Pennsylvania	1
Department of Meteorology University of California Los Angeles, California	1	Climatic Center, USAF Annex 2, 225 D Street, S.E. Washington 25, D. C.	1
Department of Meteorology University of Washington Seattle, Washington	1	Marshall Space Flight Center Aeroballistic Division Aerophysics Br (AERO-G) Huntsville, Alabama ATTN: Mr. Wm. Vaughn	1
Department of Meteorology Texas A&M College College Station, Texas	1	Comm. AFCL L. G. Hanscom Field Bedford, Massachusetts ATTN: Mr. N. Sissenwine, CRZF	1
Meteorology Department Florida State University Tallahassee, Florida	1	Director National Aeronautical Space Adm. Washington 25, D. C. ATTN: Mr. Harry Press	1